Introducing a Terrestrial Carbon Pool in Desert Bedrock Mountains

by

Emma Harrison

A Thesis Presented in Partial Fulfillment
of the Requirements for the Degree
Master of Arts

Approved April 2013 by the
Graduate Supervisory Committee:

Ronald Dorn, Chair
Mark Schmeeckle
Stephen Reynolds

ARIZONA STATE UNIVERSITY

May 2013

ABSTRACT

Growth of the Phoenix metropolitan area led to exposures of the internal bedrock structure of surrounding semi-arid mountain ranges as housing platforms or road cuts. Such exposures in the Sonoran and Mojave deserts reveal the presence of sedimentary calcium carbonate infilling the pre-existing fracture matrix of the bedrock. Field surveys of bedrock fractures filled with carbonate (BFFC) reveal an average of 0.079 +/- 0.024 mT C/m^2 stored in the upper 2 m of analyzed bedrock exposures. Back-scattered electron microscopy images indicate the presence of carbonate at the micron scale, not included in this estimation. Analysis of the spatial extent of bedrock landforms in arid and semi-arid regions worldwide suggests that ~1485 GtC could potentially be stored in the upper 2 m horizon of BFFCs. Radiocarbon dating obtained at one of the sites indicates it is likely that some of the carbonate was flushed into the bedrock system during glacial wet pulses, and is stored on Pleistocene timescales or longer. Strontium isotope analysis at the same site suggest the potential for a substantial cation contribution from weathering of the local bedrock, indicating the potential exists for sequestration of atmospheric carbon in BFFCs. Rates of carbon release from BFFCs are tied to rates of erosion of bedrock ranges in desert climates.

ACKNOWLEGEMENTS

Most importantly I acknowledge the immeasurable support and encouragement given to me by my advisor Dr. Ronald Dorn. I thank him for both his academic guidance and for introducing me to the field of study that I fell in love with.

I thank also my additional committee members, Dr. Mark Schmeeckle and Dr. Stephen Reynolds, for their important roles in my education.

To my family, Dr. Jon Harrison, Dr. Jennifer Fewell, and Michael Harrison, I am grateful to you beyond expression.

The Goldwater Environmental Laboratories at Arizona State University and Cathy Kochert for the total carbon content analysis of carbonate samples

The W.M. Keck Foundation Laboratory and Gwyneth Gordon for the strontium isotope analysis of samples

Dr. David Kinsley for BSE imagery of samples

TABLE OF CONTENTS

LIST OF TABLES

LIST OF FIGURES

Chapter 1

INTRODUCING A TERRESTRIAL CARBON POOL IN DESERT BEDROCK MOUNTAINS

INTRODUCTION

Paleoclimatic proxy records reveal that atmospheric CO_2 concentrations fluctuated between 200 and 280 ppm over the past 40,000 years, while current atmospheric CO_2 levels have now reached >100 ppm above this natural variability *(Falkowski et al., 2007)*. The historic flux of CO_2 into the atmosphere derives from short-term sources, such as fossil fuel combustion and changes in land cover biomass (*S. Liu, Bliss, Sundquist, & Huntington, 2003)*. Earth, thus, faces a pressing crisis related to atmospheric carbon dioxide management *(Sundquist, Ackerman, Parker, & Huntzinger, 2009)*.

Over geological timescales ocean-lithosphere-atmosphere carbon exchanges tended to be balanced by rates of weathering and geologic CO_2 emissions *(Sundquist, 1993)*. Decay of calcium-bearing silicates leads to geological storage of carbonates via the Urey reaction (*Urey, 1952*). This process is considered to be one of the most important for reducing atmospheric CO2 over geologic timescales of millions of years *(Berner, 2003*). However, the rate of carbon dioxide drawdown by this process has been considered too slow to be relevant to coping with the rapid modern increases in CO_2 (*Suchet, Probst, & Ludwig, 2003*). This assumption is being challenged by recent research that suggests CO_2 consumption by the weathering of carbonate minerals has been greatly underestimated and could be a principal driver of shorter-term changes in

climate *(Jacobson, Blum, & Walter, 2002)*; *(Lerman & MacKenzie, 2005)*; *(Z. Liu, Dreybrodt, & Wang, 2010); (Z. Liu, Dreybrodt, & H., 2011)*. In addition, understanding exchanges between CO_2 stored in carbonates and the atmosphere is an issue of consequence to the critical zone, the active interface between the lithosphere, atmosphere, and biota *(Amundson, Richter, Humphreys, Jobbagy, & Gaillardet, 2007)*; *(Brantley, Goldhaber, & Ragnarsdottir, 2007)*; *(Derry & Chadwick, 2007)* that stores about ~1600 Gt of organic carbon and ~900 Gt of carbon as carbonate *(Eswaran, Van den Berg, & Reich, 1993)*; *(Eswaran et al., 1999)*; *(Falkowski et al., 2007)*; *(Lal, 2004)*; (Lal, 2008); *(Schlesinger, 1982)*; *(Sundquist, 1993)*.

While carbonate in the upper few meters of the lithosphere is a relatively small element in the global carbon cycle, these deposits are both widespread and abundant, especially in what are now hyperarid, arid, and semiarid settings. These carbonate deposits exist as pedogenic calcrete *(Schlesinger, 1982)*; (Schlesinger, 1985); *(Sombroek, Nachtergaele, & Hebel, 1993)* and regolith carbonates *(Dart, Barovich, Chittleborough, & Hill, 2007)*; *(Hill, Taylor, & McQueen, 1998)*; *(McQueen, Hill, & Foster, 1999)* that include a wide range of deposits that can form through processes other than pedogenesis.

Calcium carbonate deposits infilling bedrock fractures are seen in a variety of global settings (Fig. 1). The explosive population growth in the southwestern USA, combined with the mindset of urban sprawl, has led to a great many exposures of bedrock cut through mountains and also bedrock pediments (Fig. 2), or low-relief erosion surfaces fronting ranges *(Dohrenwend*

& Parsons, 2009). Both landforms — mountain ranges and pediments — represent the same sort of carbon pool where carbonates infuse into fractures in bedrock. The focus of this paper rests in presenting initial minimum estimates about the potential magnitude of this global carbon pool. We hypothesize that the magnitude of carbonate in BFFCs could be similar to that of soil carbon pools and thus of potential relevance to atmospheric CO_2 balance on the scale of Quaternary or longer timescales.

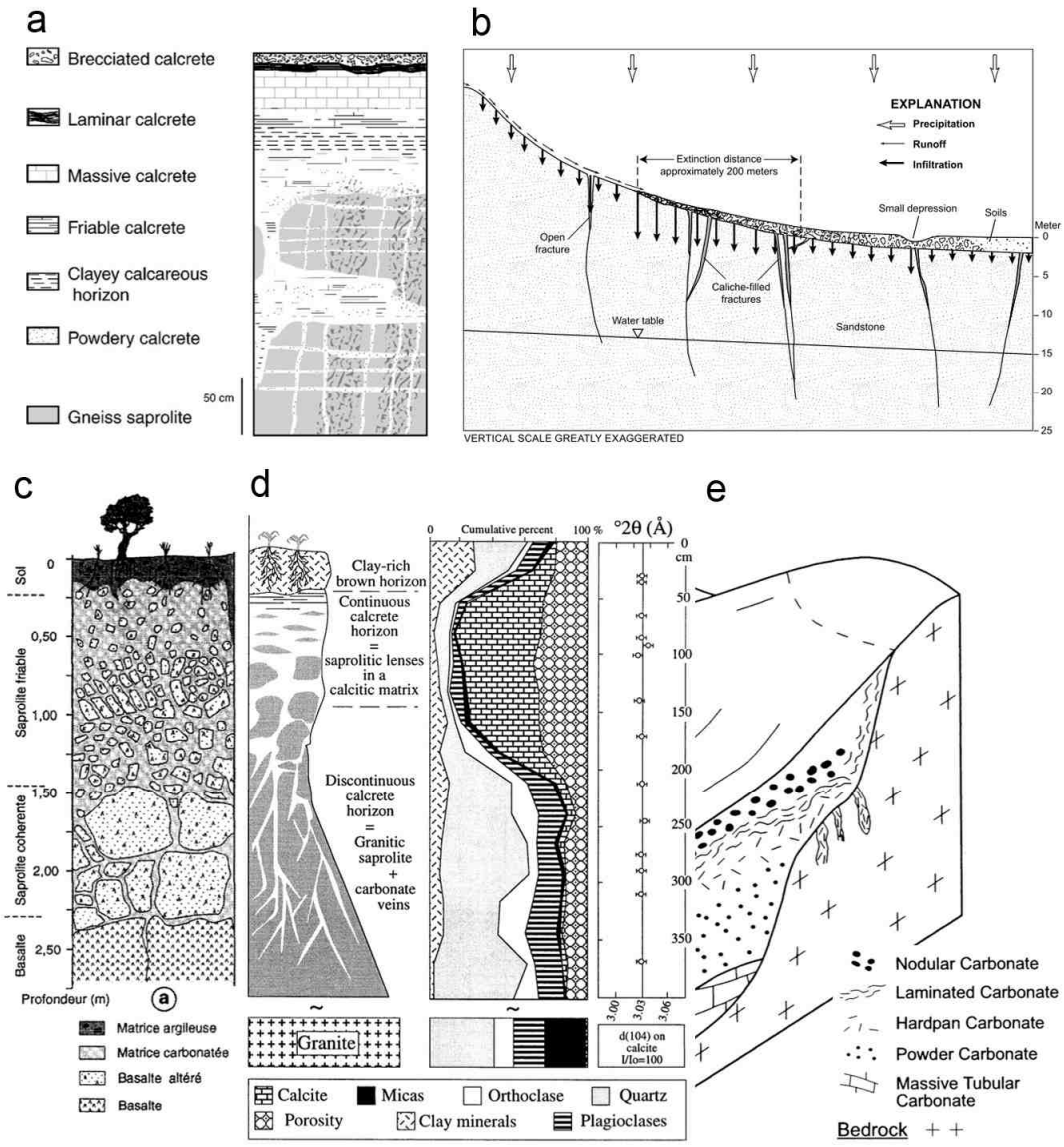

Figure 1. Diagrams showing veins of carbonate penetrating into bedrock (A) gneiss in south India *(Durand, Gunnell, Curmi, & Ahmad, 2006)* (B) sandstone in Utah, USA *(Heilweil, McKinney, Zhdanov, & Watt, 2007)* (C) basalt in the Middle Atlas of Morocco (Hamidi, Geraud, Colin, & Boulange, 1999) (D) granite in central Spain (Chiquet, Michard, Nahon, & Hamelin, 1999) and (E) varied lithologies in southeastern Australia *(McQueen et al., 1999)*. We thank the authors for permission to republish these diagrams.

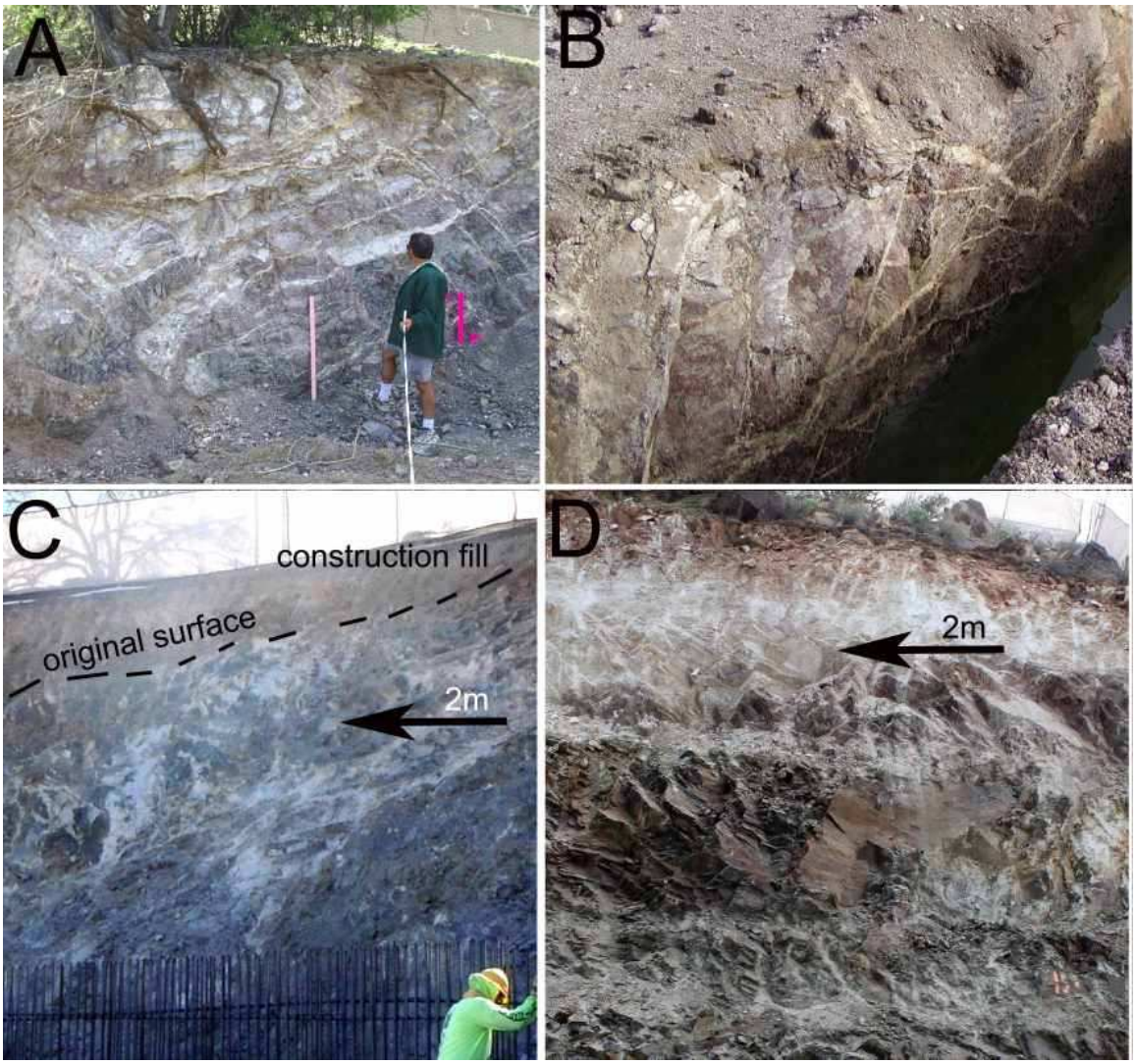

Figure 2. Views of bedrock fractures filled with carbonate exposed in metropolitan Phoenix, Sonoran Desert, Arizona: (A) orthagonal carbonate fills in diorite joints exposed in a 4 m house construction cut; (B) white carbonate fills exposed in a 3 m deep trench excavated to lay pipes; the landform is a granodiorite pediment 2.5 km distant from the adjoining range; (C) construction of a fire station water tank exposure of carbonate veins in gneiss foliations; (D) home construction exposed carbonate veins penetrating into metasedimentary rock. While most of the carbonate found in bedrock fractures occurs in the upper 2 m, penetrations can exceed 10 m.

This research follows in the footsteps of Schlesinger, who three decades ago first estimated the pool of carbon stored in the carbonate of desert soils using data from 91 Arizona soils (*Schlesinger, 1982)*, concluding that "accumulations

of pedogenic carbonate in desert soils endow these regions with a greater importance in the global carbon cycle than the amount of soil organic matter, biomass and proportional land area would otherwise suggest." (*Schlesinger, 1982*) [p. 253] For the sake of making an initial estimate, Schlesinger (*Schlesinger, 1982*) [p. 253] "assume(d) that the area of Arizona is representative of the diversity of landscapes and soils characteristics of arid and semi-arid regions of the world". Schlesinger's findings were then replicated in Arizona *(Rasmussen, 2006)* and in Spain *(Diaz-Hernandez, 2010)*. We similarly focus our efforts in Arizona and sites in the adjacent Mojave Desert of California to obtain a first rough estimate of carbon stored inside dryland bedrock.

RECOGNIZED CHARACTERISTICS OF BFFCs

Carbonate accumulates inside bedrock in arid and semi-arid environments regardless of the host rock material. BFFCs have been noted occurring in rhyolitic tuff at Yucca Mountain, Nevada, USA *(Denniston, Shearer, Layne, & Vaniman, 1997)*; *(Wilson, Cline, & Amelin, 2003)*, sandstone in Utah, USA *(Heilweil et al., 2007)*, granite in Spain *(Chiquet et al., 1999)*, gneiss in India *(Durand, Gunnell, Curmi, & Ahmad, 2007)*, different metamorphic and crystalline rocks in Australia *(McQueen et al., 1999)*; *(Quade, Chivas, & MCCulloch, 1995)*, and basalt in Hawaii *(Capo, Whipkey, Blachere, & Chadwick, 2000)*, Arizona *(Knauth, Brilli, & Klonowski, 2003)*, and Morocco *(Hamidi et al., 1999)*; *(Hamidi, Colin, Michard, Boulange, & Nahon, 2001)*. While it is certainly possible that some of the carbonate fill studied previously

(Fig. 1) could have derived, in some part, from burial history *(Winter & Knauth, 1992)*, the clear reduction in carbonate abundance with depth (Figs. 1 and 2) very likely reflects a distance decay from a surficial source of transporting meteoric fluids *(Chiquet et al., 1999)*; *(Durand et al., 2006)*; *(Hamidi et al., 1999)*; *(Heilweil et al., 2007)*; *(Knauth et al., 2003)*.

The most detailed research on carbonate veins relates to deposits at Yucca Mountain, Nevada with the premise that the carbonate informs on paleohydrological conditions *(Carlos, Chipera, Bish, & Craven, 1993)*. Drill core excavations exposed calcite deposits at depths as great as 500 m *(Vaniman & Chipera, 1996)*. These deposits "occur in open or closed fractures, cementing breccia zones, partially filling lithophysal cavities, or penetrating more porous portions of the tuff matrix" *(Vaniman & Chipera, 1996)* p.4417. In the upper ~15 m strontium isotopes *(Peterman, Stuckless, Marshall, Mahan, & Futa, 1992)* and carbon and oxygen isotope analyses (*Whelan & Stuckless, 1992)* indicated surficial sources of pedogenic carbonate. Whelan et al. (1994) obtained ^{14}C ages of 21-45 ka on eleven samples of calcite from this upper zone, and three samples with indefinite ages (*Whelan, Vaniman, Stuckless, & Moscati, 1994*). Szabo and Kyser (1990) inferred episodic calcite deposition events at 28 ka, 170 ka, and 280 ka using U-series dating (*Szabo & Kyser, 1990*). In lower stratigraphic zones, the crystal morphology of the calcites has been documented to shift from a fine-grained texture to coarser grained, tabular deposits in fractures or filling voids *(Vaniman & Chipera, 1996*). Observation that lanthanide enrichment of calcites occurs at greater depths led to the hypothesis that the sources of Ca for

the deeper calcites was hydrothermal or related to groundwater upwelling *(Bish & Chipera, 1989)*; *(Bish & Aronson, 1993)*; *(Vaniman & Chipera, 1996)*, but studies of U, Th, and Pb isotopes *(Neymark, Amelin, Paces, & Peterman, 2002)*; *(Szabo & Kyser, 1990)* and C, O, and Sr isotopes *(Neymark, Paces, Marshall, Peterman, & Whelan, 2005)*; *(Whelan, Paces, & Peterman, 2002)* have been interpreted to indicate deposition by downward percolation of meteoric water (*Stuckless, Peterman, & Muhs, 1991)*.

Whether accumulated terrestrial carbonate represents bedrock weathering or carbonate recycled from other resources has been addressed through Sr isotope ratios *(Capo & Chadwick, 1999)*; *(Chiquet et al., 1999)*; *(Dart et al., 2007)*. In these studies $^{87}Sr/^{86}Sr$ ratios of groundwater, surface water, parent bedrock material, and eolian dust are measured and compared to the $^{87}Sr/^{86}Sr$ ratios of carbonates occurring at various locations in a bedrock profile. In situations where the parent material has a high calcium content (i.e. volcanic basalts) and experiences high weathering rates, *in situ* weathering appears to be the dominant input *(Capo et al., 2000)*. In the majority of arid and semi-arid environments where Sr has been used to determine the origin of Ca in carbonate, the Ca is derived from sea spray or continental aerosols *(Capo & Chadwick, 1999)*; *(Chiquet et al., 1999)*; *(Quade et al., 1995)*.

In the Iberian Hercynian Massif of Central Spain, Chiquet *et al*. (1999) analyzed a vertical profile with a continuous calcrete horizon underlain by weathered and fresh granite infused with calcium-carbonate. The authors measured Sr isotopes of the carbonate from depths ranging from 0.01 to 3.8 m,

as well as in dust on the surface. The $^{87}Sr/^{86}Sr$ in the bedrock is much higher than the values measured in the carbonate accumulation at all depths, whereas the $^{87}Sr/^{86}Sr$ of the surface and groundwater are both within the value range for the $^{87}Sr/^{86}Sr$ of the carbonates, indicating that the primary source of calcium in the carbonate deposits is not weathering of local bedrock. With increasing depth, the $^{87}Sr/^{86}Sr$ of the carbonate samples decreases, and there is a slight increase in Ca/Sr molar ratio (a decrease in Sr concentration). The authors attribute this to a kinetic control on the precipitation rate of the carbonates by the parent material, citing a model for the genesis of calcretes based on seasonal wetting and drying of a porous parent material (*Wang, Amundson, & Trumbore, 1994*).

Analyses of carbonates at sites containing BFFCs in Morrocco and Australia reveals only minor uptake in CO_2 from bedrock weathering (*Dart et al., 2007*); *(Hamidi et al., 2001)*. In contrast, about 55% of the carbonates deposited in the early Holocene and late Pleistocene in South India derive from local gneiss. Knauth et al. (2003) find "there is apparently a significant amount of Ca that is not of wind-blown origin in these young basalts" (*Knauth et al., 2003*) [p.189]. Previous research has also demonstrated an affinity for carbon drawdown by weathering of basalt (*Torn, Trumbore, Chadwick, Vitousek, & Hendricks, 1997)*.

Despite the diverse interest in BFFCs presented in this brief review, no prior research has attempted to estimate the amount of carbon stored inside the bedrock of mountains and pediments in drylands, where low precipitation levels

produce abundances of calcium-carbonate in the pedogenic environment (*Schlesinger, 1982*)

SOUTH MOUNTAIN SITE DESCRIPTION

The foothills region of the Gila Range in the South Mountain Metamorphic Core Complex in Maricopa County, central Arizona was selected for a preliminary investigation of the sources of the carbonate and the age of the deposits (Fig. 3). This site was selected for several reasons. The climatic conditions in the subtropical Sonoran Desert generally contains precipitation levels high enough to mobilize carbonate from bedrock and dust, but infiltration rates are low enough so that the carbonate is not fully flushed to groundwater. The geology of the Gila Range is fairly homogeneous, consisting of Early Proterozoic mostly gneissic with some metavolcanic rocks. The homogeneity is important, because of the need for random selection of study sites. Pragmatically, the foothills of the Gila Range of South Mountain host an exceptional number of deep and relatively fresh road cuts that were excavated in the process of developing the Ahwatukee suburb of Phoenix, Arizona.

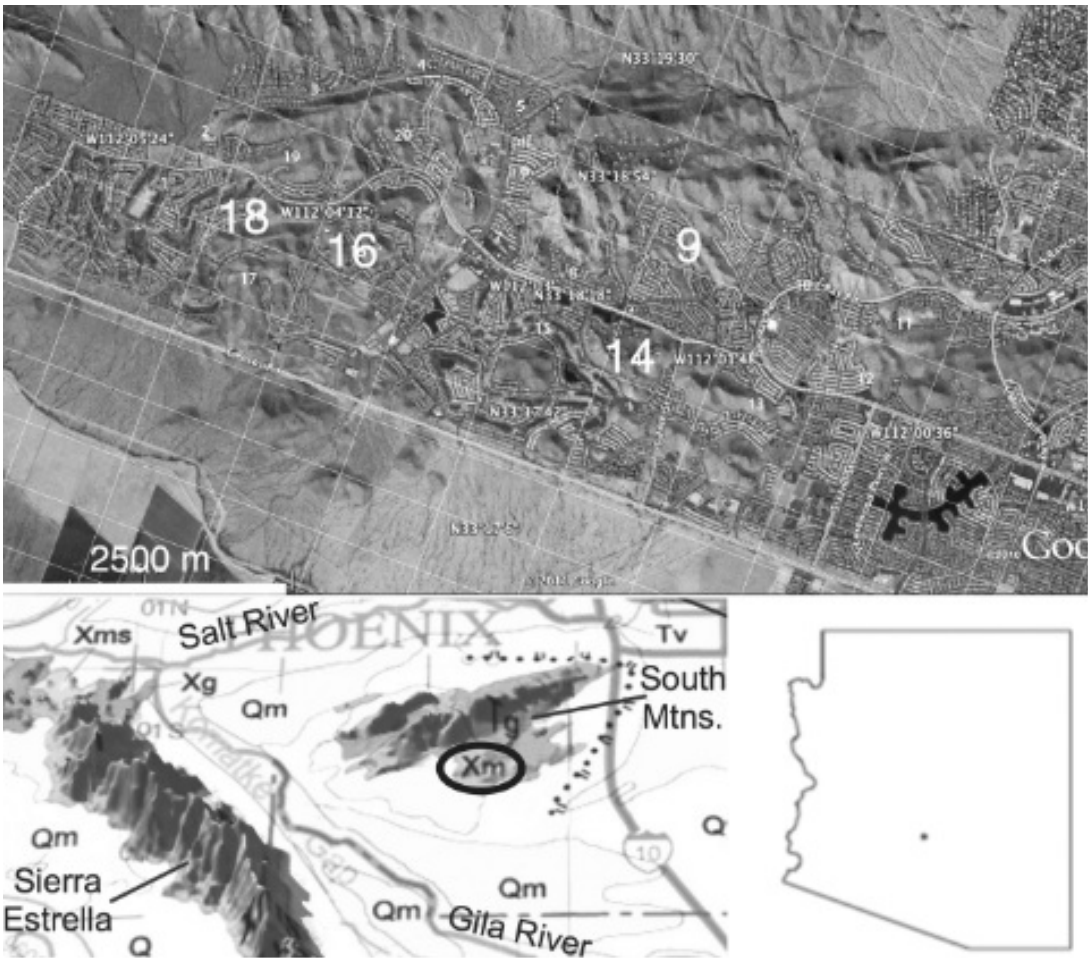

Figure 3. *Study site of the Gila Range foothills of South Mountains, central Arizona. The geological map of the area (Reynolds & Bartlett, 2002) shows the Xm (circled area) Early Proterozoic gneissic and metavolcanic rocks of the Gila Range and the foothills area. The "Xm" lettering on the geological map delineates the area of the aerial photograph (The image follows permission guidelines for Google Earth, http://www.google.com/permissions/geoguidelines.html).*

Figure 2. Study site of the Gila Range foothills of South Mountains, central Arizona. The geological map of the area (Reynolds & Bartlett, 2002) shows the Xm (circled area) Early Proterozoic gneissic and metavolcanic rocks of the Gila Range and the foothills area. The "Xm" lettering on the geological map delineates the area of the aerial photograph (The image follows permission guidelines for Google Earth, http://www.google.com/permissions/geoguidelines.html).

The importance of cleanly exposed bedrock cannot be underestimated, given that BFFCs are only seen naturally in locations of active bedrock erosion. Encroachment of neighborhood development is responsible for the production of road-cuts by bulldozer action and dynamite. Road cuts are ideal for this study

because they provide perspective of the bedrock composition at different depths viewed as a cross section.

For a road cut to be a study site in this research, it had to adhere to pre-determined criteria. First, it is important that a cut be exposed within the last fifteen years, so that the carbonate would not have dissolved through interaction with carbonic acid in precipitation, and so that the exposure is not obscured by weathered materials and vegetative cover. Second, the road cut should be a minimum of 2 meters in height in order to understand variations with depth. Third, there must be a reasonably safe access route to the upper 2 meters of the cut. Road cuts adjacent to busy main roads or highways are excluded from consideration based on potential hazards.

To select the sample site that meet the aforementioned criteria, I employed 3-steps in random stratified sampling of road cuts. Step 1 grids communities in the foothills section of the Gila Range into different field regions using a Google Earth image as a base map. Step 2 assigns grid squares within the foothills section numbers. Then, a random number generator selects four grid squares. Step 3 involves locating the road cut that is closest to the center point of the randomly selected grid cell that adheres to the aforementioned criteria for road cuts as sample sites. The selected grid cells 5, 9, 16 and 17 correspond with study sites (Fig. 3):

Cabrillo Canyon (N 33.31543 W 112.04327)

Liberty Lane (N 33.29621 W 112.03433)

3rd and Frye (N 33.30074 W 112.07014)

Marketplace (N 33.30725 W 112.06160)

Out of these four randomly selected sites, the Marketplace site met a key fourth criteria: that the site was in a location where "digging back" into the exposure would create a minimal disturbance. In the case of the Marketplace site (Fig. 4), the exposure had a small trench at the bottom that could accept anthropogenic spalling with little impact. The sampled exposure (Fig. 5) exposure displays carbonate infilling the existing bedrock fracture matrix at depths of up to 3 meters as veins ranging from a millimeter to meters in thickness.

Figure 4. *Oblique aerial photograph showing the context of the Marketplace study site, randomly selected for this study. The bedrock fractures filled with carbonate can even be seen as bright lines from a flying altitude of about 1000 m above the surface.*

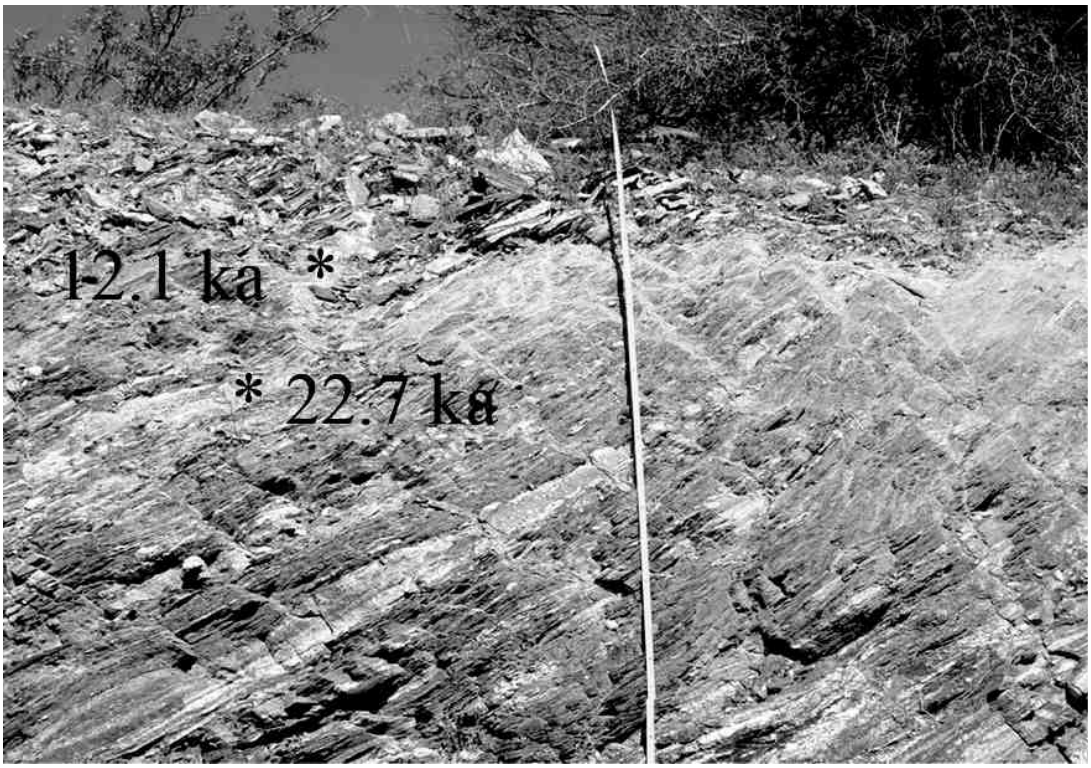

Figure 5. *Upper 2.8 m of the Marketplace exposure, where asterisks indicate the location of sample collection for the radiocarbon ages — reported in calendar years BP.*

Samples from this exposure were collected at depths of one and two meters from a carbonate vein for radiocarbon dating. Samples of bedrock and of vein carbonate 30 cm back into the exposure were collected at depths of one, two, and three meters for comparative strontium isotopic analysis.

STRONTIUM ISOTOPES AS PROVENANCE INDICATORS

Measurements of the abundance of carbon resting in BFFCs in the Sonoran and Mojave Deserts reveal the possibility that BFFCs might be a sink for carbon on the order of magnitude of soil organic matter. The implication of BFFCs for the global carbon cycle depends on the origin of the carbonate being stored in these bedrock fractures. One potential source would be the decay of

calcium-bearing silicates via the Urey reaction *(Urey, 1952)*. While rates of carbon dioxide drawdown through the decay of Ca-silicates is probably too small to ameliorate rapid modern increases in CO_2 *(Suchet et al., 2003),* storage of carbon dioxide in BFFCs could be a player in explaining some Quaternary CO_2 fluctuations.

A second potential source of the carbonate stored in BFFCs would be dust, where mobilization of dust-borne carbonate into bedrock fractures represents recycling of carbonate in the terrestrial critical zone. If this is the case, some research argues that the decay of carbonate minerals could be a driver of shorter-term changes in climate *(Jacobson et al., 2002); (Lerman & MacKenzie, 2005); (Z. Liu et al., 2011); (Z. Liu et al., 2010)*. Thus, the ongoing storage and dissolution of recycled carbonate in BFFCs could play a role in climate change.

The general strategy to understand the origin of calcium found in calcium carbonates is to use strontium isotopes, because Sr sometimes replaces calcium in carbonate. Ratios of $^{86}Sr/^{87}Sr$ in carbonate are useful indicators of cation provenance, because $^{86}Sr/^{87}Sr$ ratios of surficial carbonates represent a fingerprint of the various sources to the sediment. The relative inputs of allochthonous sources such as local bedrock, meteoric water, atmospheric dust, ground water, surface water, and sea-spray can be assessed by using a mixing equation in conjunction with strontium isotope measurements. Equation *1.1* determines the relative input of sources to a reservoir:

$$\delta_{\text{mix}} = \frac{M_1^{\text{Sr}}\delta_1 + M_2^{\text{Sr}}\delta_2 + \ldots + M_n^{\text{Sr}}\delta_n}{M_1^{\text{Sr}} + M_2^{\text{Sr}} + \ldots + M_n^{\text{Sr}}}$$

In a two-component system, the relative contribution of components is calculated by equation *1.2*:

$$\frac{M_1^{Sr}}{M_1^{Sr} + M_2^{Sr}} = \frac{\delta_{mix} - \delta_2}{\delta_1 - \delta_2}$$

Soil carbonates are typically approached using the second equation. The contributing sources are 1) accumulation from eolian deposition or 2) as a result of weathering of silicate minerals, described by the "Urey Reaction" (*Urey, 1952)*:

$$CO_2 + CaSiO_3 \leftrightarrow CaCO_3 + SiO_2$$

The general finding of Sr studies of soil carbonate is the calcrete has been recycled from eolian dust. For example, (*Capo & Chadwick, 1999)* found ~98% of carbonate in a petrocalcic soil horizon above granitic bedrock in New Mexico was of eolian origin. In another example, (*Quade, Chivas, & MCCulloch, 1995)* reports ocean spray is the principal source in coastal soils in Australia progressively influenced inland by continental dust, with the exception of one region where weathered volcanic ash is the primary cation-producing agent. However, this is not always the case. (*Capo, Whipkey, Blachere, & Chadwick, 2000*) found that weathering generated more than 75% of carbonate developed on basaltic soils in Hawaii. In a study of a complex carbonate profile that mixes soil carbonate and some BFFCs (Fig. 1D), (*Chiquet, Michard, Nahon, & Hamelin,*

1999) calculated that decay of granite bedrock contributed between 3% and 33% of the pedogenic carbonate reservoir in the Toledo Mountains, central Spain.

These studies differ from the one presented here because they focus on carbonate incorporated into soil or regolith profiles. Few studies have explored calcium carbonate deep in bedrock fractures. These deposits are unique from pedogenic carbonate because theoretically they exist as closed systems. Weathering and dust deposition occurs at the surface, but the physical processes impacting the deeply penetrating carbonates are significantly restricted. Thus, isotope indicators ought to be reflective of the conditions present at the time of emplacement.

The majority of studies addressing penetrative carbonates at depth occurred at Yucca Mountain, Nevada, during consideration for use as a nuclear waste repository. (*Vaniman & Whelan, 1994*) report carbonates "penetrating about 15 m into fractures and faults" at the location. These carbonates were analyzed for hydraulic interaction by groundwater and meteoric waters as a means for assessing hydraulic interactions with stored hazardous material. Sr isotope ratios and U-series dating by (*Neymark, Paces, Marshall, Peterman, & Whelan, 2005*) and (*Stuckless, Peterman, & Muhs, 1991*) determined that the carbonate were not derived from upwelling of the local water table. Stable ^{13}C and ^{18}O isotopes were determined for soil carbonates by *(Quade, 1990),* (*Vaniman & Whelan, 1994)* and *(Neymark et al., 2005)* indicate that the deposits were formed by the evaporation of downward percolating meteoric water. Quade and Cerling

(1990) report the carbonates "likely formed in the presence of vegetation and rainfall typical of a glacial climate".

$^{86}Sr/^{87}Sr$ ratios are presented for calcium carbonate deposits infilling deeply penetrative fractures in the South Mountains, Arizona. The isotope ratios of carbonate samples collected from inside fractures are compared to the isotope ratios of the bedrock gneiss encasing it. The purpose of the investigation is to evaluate the potential impact for carbon sequestration of carbonate infilling bedrock fractures. The results of the preliminary data indicate that a substantial proportion of the carbonate could be derived from weathering of local gneiss.

Chapter 2

METHODS

To estimate the carbon pool of BFFCs in southwestern desert mountains, we first located recent excavations. Recent exposures are important, because the friable nature of the carbonate results in flaking that reduces measured values over time. Second, the portion of the cut analyzed was selected through an objective process (see below), so that sampling did not favor exposures either reduced or relatively enriched in BFFCs. Third, we estimated the percent C and density of the BFFCs are measured from randomly collected samples in the excavations. Lastly, the C content of samples within sites was converted to a basic unit of mT C/m^2.

In addition to compiling the first estimate of the storage of carbon in desert bedrock, we conducted back-scattered electron (BSE) microscope studies

to examine whether BFFCs are stored in fractures smaller than studied through fieldwork. An additional goal of the BSE study was to look for textures that would suggest post-depositional diagenesis *(Bathurst, 1972)*; *(Chitale, 1986)*; *(Klappa, 1979)*; *(Moore, 1989); (Nash & McLaren, 2003)*; *(Stokes, Nash, & Harvey, 2006)*; *(Verrecchia, 1990)*; *(Watts, 1980)*. We analyzed radiocarbon in samples where BSE textures did not show evidence of post-depositional diagenesis, based on our assumption that ^{14}C values reflects the actual timing of deposition of laminated carbonate.

To investigate the sources of carbonate to BFFCs samples of unexposed carbonate were collected by digging back ~30 cm into the exposure face. The unexposed carbonate, samples of the local bedrock, and carbonate in dust infusing fractures in the exposed bedrock were analyzed for $^{86}Sr/^{87}Sr$ isotopic ratios. The comparison between the samples provides preliminary data suggesting a possible input by weathering of the local bedrock.

MEASUREMENT OF CARBONATE ABUNDANCE IN EXCAVATIONS

This study pools data from a quarter century of examining excavations made by bulldozers at Sonoran and Mojave Desert sites. These excavations come in all different dimensions (e.g. Fig. 2) including small exposures associated with home construction, long and shallow exposures during road construction, and deep excavations for such features as water towers.

A comparison of different sites requires a common depth of measurement. We decided to focus on the upper 2 m for a few reasons. First,

many excavations did not go significantly deeper than 2 m, so using this depth greatly increased the number of excavation sites that could be compared. Second, prior studies have suggested that carbonate contents decline strongly at depths below 2 m *(Chiquet et al., 1999)*; *(Durand et al., 2006)*; *(Heilweil et al., 2007)*; our results support this conclusion.

We used two different strategies to randomize the particular exposure of 20 m^2 analyzed at an excavation, based on the amount of exposed bedrock. In circumstances such as a subdivision with abundant road cuts, a stratified random sampling approach was used to select the study sites. First, the subdivision was divided into grids, and random number generator was used to select grid squares to be analyzed. Second, within the grid, we selected the bedrock exposure closest to the center point of the grid that adhered to specific criteria: (i) an exposure that has not been obscured by weathered materials or vegetative cover; (ii) a minimum of 2 m in height and 10 m in length; and (iii) safe access. When exposures had more than 20 m^2 of exposure, we analyzed the "cleanest" 20 m of exposed cross-section (least vegetation/fill covering, and most regular surface).

We also used two approaches to measure the percent of BFFCs found in bedrock fractures. During the early years of data collection for this study, rolls of gridded plastic were pinned to exposures. Markers mapped out BFFCs with widths greater than 3 mm on the grids, that were then counted manually and a percentage calculated for an excavated exposure of 20 m^2. During later years of data collection, we used digital image processing of high resolution visual images. Carbonate veins were manually mapped as a separate "layer" in a photo

editor. Then, this mapping was rechecked in the field to minimize the chance of mis-mapping features like igneous veins or quartz-rich foliations as carbonate. Then, after field rechecking, BFFC maps were processed as separate images. This black and white map of BFFC veins enables the calculation of percent area of BFFC with NIH Image software (Fig. 6). These manual and automated procedures generated an overall percent of bedrock occupied by carbonate veins in 31 different locales in the Sonoran and Mojave Deserts, southwestern USA, with coordinates presented in Table 2.

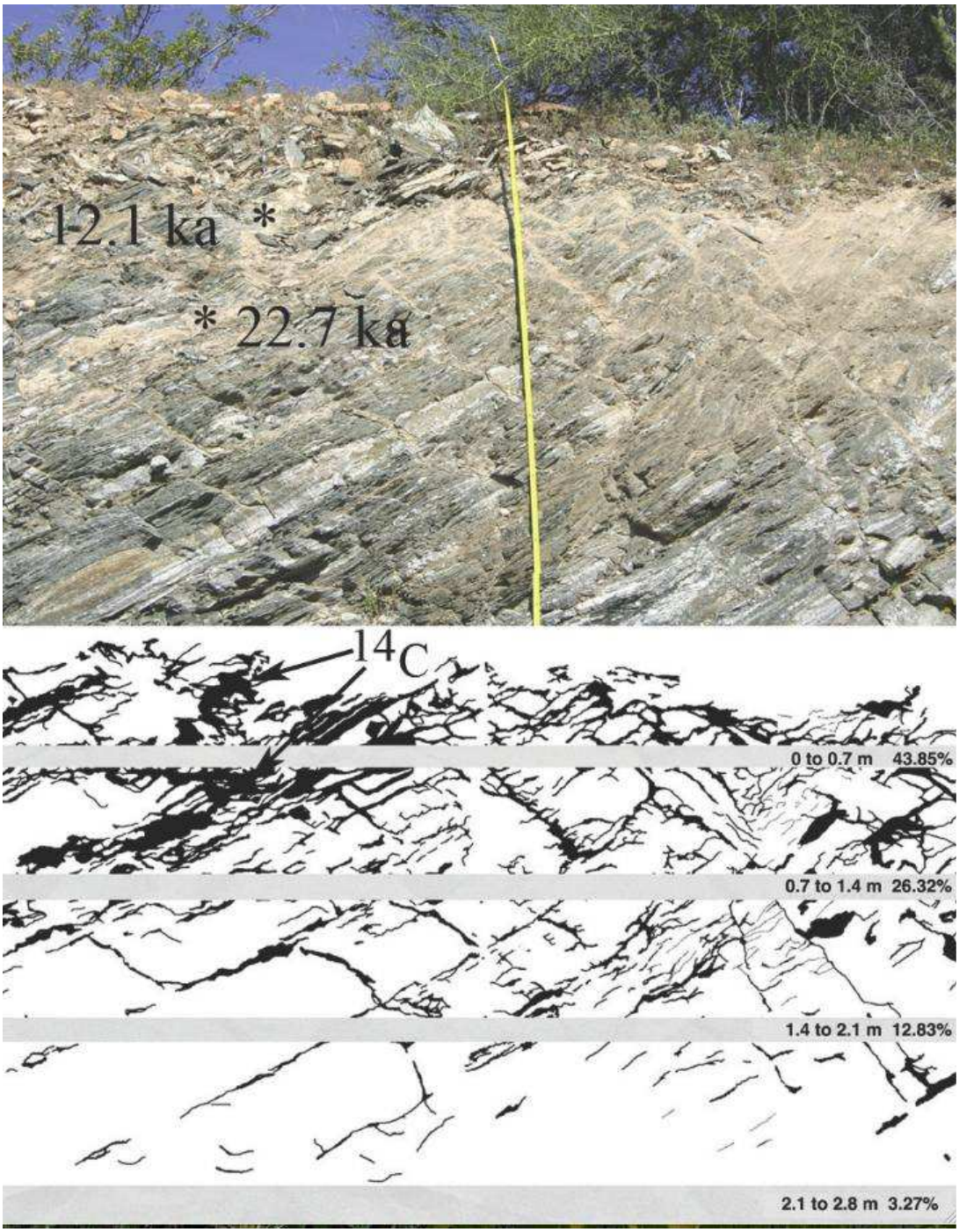

Figure 6. Road excavation cut into the Gila Range, central Arizona, where digital image processing generated a map of the carbonate veins in bedrock. Asterisks indicate the location of radiocarbon samples collected from a vein. Note the higher cross-sectional area percentages of carbonate closest to the surface. The colluvium and soil is not a part of the carbonate mapping; mapping of the fractures filled with carbonate only occurs in the area of exposed bedrock.

Since bulldozers do not generate cubes, the assumption made for each site is that 2D percentages acquired for an excavation are valid approximates for 3D percentages of carbonate infused into bedrock. We were able to assess this assumption at three different sites where a bedrock excavation made turns approximating a right angle: Scottsdale Mountain, Golden Eagle 2, and Las Sendas sites in Table 2. At these locations three sides of a rectangular solid were analyzed for the percent carbonate exposed in a cross-section.

Carbonate deposited inside bedrock fractures can be quite friable. While we made every attempt to collect data from sites recently dynamited or bulldozed, some sites were not identified until years after excavation. Thus, in order to understand if abundances would decrease over time in an exposure and bias findings, we returned to four exposures (Golden Eagle 1, Golden Eagle 2, Gold Canyon 1, Gold Canyon 2) years after the initial study of a site. The return visit then led to a new measurement of the percent of exposed carbonate and a better understanding of how the abundance in a bedrock exposure can change over time.

MEASUREMENT OF PERCENT CARBON AND SAMPLE DENSITY

Ten samples were collected from each exposure, typically along two veins at depths of 0.4, 0.8, 1.2, 1.6 and 2.0 m. These samples were split for analysis of the percent carbon and sample density. The samples were analyzed at the Goldwater Environmental Laboratories at Arizona State University by a Perkin-Elmer elemental analyzer to determine the weight percent carbon.

Density (g/cm^3) was measured by determining the volume of weighed sample from the displacement of water in graduated cylinders.

CALCULATION OF CARBON ABUNDANCE

For each site in Table 2, the quantity of C per square meter of surface to a depth of 2 meters was calculated as:

$$[1] \qquad C/m^2 = bvCD$$

where

- b - the percent of bedrock fracture fills composed of calcium carbonate in the upper 2 meters of a bedrock exposure
- v – volume in cm^3 of a rectangular solid that is 2 meters deep with a surface area of 1 m^2 , or 2 x 10^6 cm^3
- C – carbon content of the BFFCs at a site, measured in percent C by weight
- D – density of the BFFCs

Densities of carbon were reported as mT C/m^2.

The standard deviations of the percent C and density propagates into the error term of mT C/m^2 for each site. One standard deviation of the average of percent C and density generates the reported standard deviation of mT C/m^2 using equation 1.

ELECTRON MICROSCOPE ANALYSIS

Back-scattered electron (BSE) microscopy generates gray-scale images of average Z from polished cross-sections. Bright portions of the image reflect a higher atomic number (*Krinsley & Manley, 1989*). Energy dispersive X-ray spectrometry (EDS) provides elemental data of the different micron-scale areas

visualized through the BSE detector (*Goldstein et al., 2003*). We employed BSE and EDS in three separate investigations.

The field-based methods used to measure carbon abundance at sites in Table 2 only analyze veins of carbonate wider than 3 mm. This means that all veins smaller than 3 mm are not included in the reported values. In order to investigate the possibility that carbonate infuses into bedrock in submillimeter veins, samples of bedrock without any visually apparent carbonate veins were collected from depths of 0.2, 0.4, 0.6, 0.8, 1.0, 1.2, 1.4, 1.6, 1.8, and 2.0 m from the Las Sendas site imaged in Fig. 2A. Then, for each sample, a cross-sectional area of 1.0 mm^2 was polished and analyzed through acquisition of multiple images at a magnification of 1000x; EDS was employed to identify carbonate. Then, digital image processing quantified the percent carbonate at each of these depths, using methods described elsewhere (*Dorn, 1995*). This approach generates a profile of changes in percent carbonate with depth in samples that had no visually apparent presence of a BFFC.

The second use of BSE and EDS involved a qualitative study of BSE textures of the BFFC samples. One sample from a depth of 1m in one vein from each site in Table 2 was turned into a polished cross-section. Textures indicative of post-depositional diagenesis were observed in several samples Fig. 7. The third use of BSE relates to the next section on radiocarbon dating.

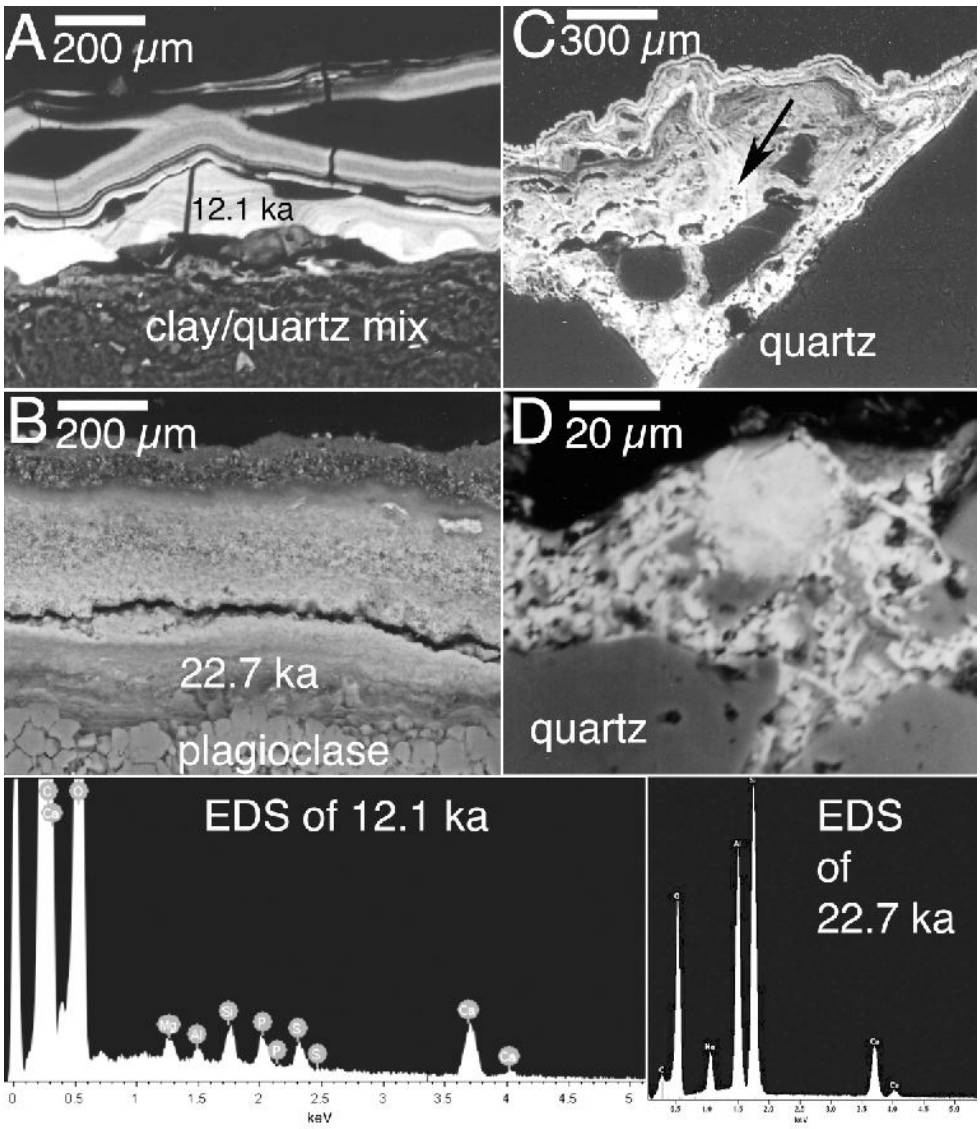

Figure 7. BSE imagery of laminar textures used in ^{14}C (A and B) and non-laminated textures avoided (C and D) for ^{14}C dating (see **Fig. 6** for field context). The laminar texture in image A separated nicely from the weathered sidewall of the fracture and from the overlying silica-rich (darker) layer in sample scraping with a tungsten-carbide needle. The dated laminar texture in image B is darker than the overlying granular layer, because it contains some clay minerals (Na, Al, Si in the EDS spectra). The overlying granular layer had to be physically abraded away with a Dremel drill in order to separate it from the underlying laminar texture. We explicitly avoided textures showing remobilization of carbonate (e.g. arrow in image C showing cross-cutting reprecipitation) and mixed textures of silica and carbonate (image D) suggestive of ongoing diagenesis through silica substitution.

RADIOCARBON DATING

Soil carbonate is fraught with uncertainties in obtaining reliable ^{14}C results with post-depositional diagenesis a key concern *(Callen, Wasson, & Gillespie, 1983)*; *(Stadelman, 1994)*; *(Wang et al., 1994)*. The apparent ^{14}C age could be altered when small amounts of capillary water remobilize carbonate. Thus, because it is essential to recognize different carbonate fractions (*Candy, Black, Sellwood, & Rowan, 2003*); *(Fletcher, Rockwell, & Sharp, 2011)* we worked with samples that reflect the initial deposition of laminar calcrete.

We collected two samples for radiocarbon dating from the Gila Range site in Fig. 6. The samples were collected from the same vein, at depths of 0.4 m and 0.8 m. BSE was used to identify portions of the samples that had a laminar texture (Fig. 7). The laminated carbonate was submitted to Beta Analytic for conventional radiocarbon dating.

STRONTIUM ISOTOPE RATIOS

Three different types of samples were collected for analysis (Table 1). The principal target is the $^{86}Sr/^{87}Sr$ isotopic ratio of the carbonate veins that exist infilling the fracture matrix of the bedrock mountain. Samples of this carbonate were collected 30 cm into the exposure face to avoid contamination by dust and meteoric water. Samples of gneiss were collected from the exposure to be analyzed as a potential source for the carbonate. The gneiss was leached with HCl prior to analysis. The leachate represents carbonate dust blown around and

infused into the fractures of the gneiss after the roadcut was created. This leachate was also analyzed.

Table 1. Descriptions of samples for Sr isotope analysis

Sample Code	Sample description
G R1	Gneiss Replicate 1, HCl leached
G R2	Gneiss Replicate 2, HCl leached
G R3	Gneiss Replicate 3, HCl leached
G UL	Gneiss Replicate 4, no HCl leaching
GSC MG	Gneiss Leachate Carbonate, combined from GR1, GR2 and GR3
SAC V1	BFFC vein, 30 cm into the exposed face
G SZ	Gneiss, HCl leached
GSC SZ	Gneiss Leachate Carbonate
SAC V2	BFFC vein, 30 cm into the exposed face
G LP	Gneiss, HCl leached
GSC LP	Gneiss Leachate Carbonate
SAC V3	BFFC vein, 30 cm into the exposed face
G2	U.S.G.S. granite standard (Balcaen, 2005)
SRM987	Standard run for the mass spectrometer
SRM987	Standard run for the mass spectrometer

The bedrock samples were leached with dilute HCl, then reduced to a fine powder with a ball mill. The powdered material was digested in several steps of dilution with hydrofluoric and nitric acid, and with hydrochloric acid. The carbonate vein samples were digested in hydrochloric acid. Once in solution the gneiss, carbonate veins, and leachate carbonate were passed through strontium columns and prepared for chemical analysis.

The concentration of ^{85}Rb, ^{84}Sr, ^{86}Sr, ^{87}Sr, and ^{88}Sr were measured with the Thermo Neptune MC-ICP-MS. The $^{86}Sr/^{87}Sr$ ratios measured are presented in Table 2. An unresolved issue with the sample introduction system is reflected in a deviation from the known values of the standards that were analyzed. While it is

unlikely that this issue substantially interrupts the trends collected by the analysis, these data will remain unpublished until a correction can be made.

Chapter 3

RESULTS

ABUNDANCE OF CARBON AT SONORAN AND MOJAVE DESERT EXCAVATION SITES

Values of mTC were generated for the upper two m of 31 excavations in the Sonoran and Mojave Deserts. The sites consist of different rock types, ranging from basalt to sandstone. Locations include 24 excavations into bedrock hillslopes and 7 excavations of bedrock pediments. The percent of the excavation area consisting of calcium carbonate veins averaged 23.3% and ranged from 5.2% to 42% (Table 2). The percent carbon averaged 8.4% (range 7.3-10), and was consistently less than the expected value of 12% for calcite (Table 2). The density of the samples averaged 1.4 g/cm^2 (range 0.5-2.0), less than the expectation for calcite of 2.71 g/cm^2 (Table 2). The total mass of carbon in these desert mountains averaged 0.079 mT/m^{-2}, ranging from 0.015-0.139 (Table 2).

Table 2. Metric tons of carbon observed at excavations of bedrock in the Sonoran and Mojave Deserts.

Site	Rock (**H**illslope or **P**ediment)	Coordinates	% $CaCO_3$	% C	± SD	g/cm^3	± SD	$mTCm^2$	± SD
303 Site 1 *	Basalt (H)	N 33.75193 W 112.29585	20.64	8.04	± 1.58	2.00	± 0.33	0.066	± 0.022
303 Site 2 *	Sandstone & Breccia (H)	N 33.76538 W 112.28804	5.23	7.27	± 1.35	1.92	± 0.34	0.015	± 0.005
Adobe Mountain	Basalt (H)	N 33.69376 W 112.11642	38.40	7.97	± 1.62	2.08	± 0.31	0.127	± 0.041
Anthem	Metavolcanic (H)	N 33.86550 W 112.09160	12.77	9.43	± 1.79	1.79	± 0.30	0.043	± 0.014
Anthem	Metavolcanic (P)	N 33.86550 W 112.09160	19.35	8.85	± 1.51	2.10	± 0.27	0.072	± 0.020
El Paso Gas Pipleline Site 1	Metasediment ary (H)	N 33.97452 W 112.13994	14.44	8.79	± 1.41	2.11	± 0.30	0.054	± 0.015
El Paso Gas Pipleline Site 2	Granitic (H)	N 34.13584 W 112.15820	23.01	9.07	± 1.24	2.03	± 0.31	0.085	± 0.023
El Paso Gas Pipleline Site 3	Basalt (H)	N 34.29871 W 112.17479	37.22	8.33	± 1.49	1.97	± 0.38	0.122	± 0.041
Estrella Mountain Ranch	Granitic (H)	N 33.29646 W 112.42709	26.07	9.31	± 0.56	2.04	± 0.41	0.099	± 0.025
Estrella Mountain Ranch	Granitic (P)	N 33.29646 W 112.42709	39.55	8.68	± 1.32	1.89	± 0.34	0.130	± 0.040
Fountain Hills	Breccia (H)	N 33.58870 W 111.73826	6.65	7.89	± 1.89	1.83	± 0.29	0.019	± 0.007
Gila Foothills	Gneiss (H)	N 33.30636 W 112.06145	32.58	8.71	± 1.76	2.45	± 0.32	0.139	± 0.043
Gold Canyon 1	Ignimbrite (H)	N 33.37596 W 111.44589	9.44	8.25	± 1.12	2.19	± 0.28	0.034	± 0.008
Gold Canyon 2	Ignimbrite (H)	N 33.37059 W 111.45409	13.22	7.88	± 1.69	2.13	± 0.33	0.044	± 0.015
Gold Canyon 2	Ignimbrite (H)	N 33.37219 W 111.46714	21.48	8.16	± 1.42	2.06	± 0.27	0.072	± 0.020
Golden Eagle 1	Metasediment ary (H)	N 33.63841 W 111.77947	42.06	8.47	± 2.02	1.86	± 0.28	0.133	± 0.047
Golden Eagle 2	Metasediment ary (H)	N 33.63888 W 111.77404	17.66	8.90	± 1.16	2.04	± 0.27	0.064	± 0.016
Hedgpeth Hills	Basalt (H)	N 33.68186 W 112.17058	37.29	7.95	± 1.92	1.87	± 0.35	0.111	± 0.043
Hwy 58 Site 1	Granitic (P)	N 35.01643 W 117.97553	25.03	8.02	± 1.45	1.98	± 0.35	0.079	± 0.026
Hwy 58 Site 2	Granitic (P)	N 35.01791 W 118.00115	32.19	8.51	± 1.49	2.05	± 0.33	0.112	± 0.035
Las Sendas	Granitic (H)	N 33.48364 W 111.67462	24.06	10.06	± 0.65	1.95	± 0.34	0.094	± 0.021
Las Sendas	Granitic (P)	N 33.48462 W 111.67494	35.29	8.46	± 1.25	2.17	± 0.31	0.130	± 0.035
Lost Canyon	Metavolcanic (H)	N 33.69334 W 111.85147	16.37	7.32	± 1.38	2.02	± 0.31	0.048	± 0.015
San Tan Site 4	Metasediment ary (H)	N 33.19670 W 111.64982	18.78	8.05	± 0.95	2.11	± 0.36	0.064	± 0.017
SanTan Site 1	Granitic (H)	N 33.15223 W 111.61566	18.65	8.40	± 1.47	2.08	± 0.28	0.065	± 0.019
SanTan Site 2	Granitic (P)	N 33.16001 W 111.62084	22.56	7.90	± 1.66	2.20	± 0.20	0.078	± 0.022
SanTan Site 3 *	Sandstone (H)	N 33.11868 W 111.64126	6.41	8.41	± 1.71	2.22	± 0.36	0.024	± 0.008
Scottsdale Mountain	Metasediment ary (H)	N 33.60866 W 111.78678	14.00	7.96	± 1.42	2.05	± 0.38	0.046	± 0.015
Stetson Hills *	Basalt (H)	N 33.72153 W 112.14762	34.91	8.51	± 1.46	1.98	± 0.28	0.118	± 0.034
Verado	Granitic (H)	N 33.48444 W 112.51255	20.55	8.16	± 0.90	2.13	± 0.27	0.071	± 0.016
Verado	Granitic (P)	N 33.48444 W 112.51255	36.11	8.70	± 1.08	1.67	± 0.40	0.105	± 0.035

* Vertical cross-sections were not available. At these sites, construction activity exposed bedrock parallel to the former surface. These study locations occur 0.5 meters beneath the former bedrock hillslope surface.

VARIATION IN 3D EXPOSURES

The assumption that 2D excavations generate similar abundances of carbon as 3D rectangular blocks was assessed at three different sites in Table 1. At Scottsdale Mountain, sides 1, 2 and 3 of a rectangular solid displayed abundances of carbonate of 12.35%, 13.70%, and 15.95%. At Golden Eagle Site 2, sides 1, 2 and 3 of a rectangular solid displayed abundances of carbonate of 18.69%, 15.04%, and 19.25%. At Las Sendas, sides 1, 2 and 3 of a rectangular solid displayed abundances of carbonate of 21.55%, 24.51%, and 26.04%. These measurements, while not statistically significant, suggest that measurements of any given exposure with provide an estimate within ~15% of the average three-dimensional content.

CARBONATE EROSION FROM EXCAVATIONS

Our repeated measurements of carbonates over time clearly indicated that carbonate content of faces declined strongly with time after excavation. Golden Eagle sites 1 and 2 were revisited 1, 2 and 3 years after the initial study of an excavation analyzed within a week of bulldozing. The percent carbonate declined from 42.06% to 33.19% in three years at Golden Eagle 1. At Golden Eagle 2, the decline was from 17.66% to 3.88%.

Gold Canyon sites 1 and 2 were revisited 5 and 10 years after the initial study of an excavation that was studied 2 years after construction. The percent carbonate at Gold Canyon 1 declined from 9.44% to 1.81% five years later, and

down to 0.50% ten years after the first measurement. At Gold Canyon 2, the 13.22% declined to 5.05% after five years and to 1.20% after ten years.

ABUNDANCE OF CARBONATE IN MICRO-VEINS

A BSE investigation of micrometer-scale fractures at the Las Sendas site (Fig. 2A and Table 2) reveals that calcium carbonate comprised about one percent of rock area (Fig. 8). These samples showed no visual evidence of BFFC penetration when collected in the field. At this site, the abundance of micro-carbonate declined with depth.

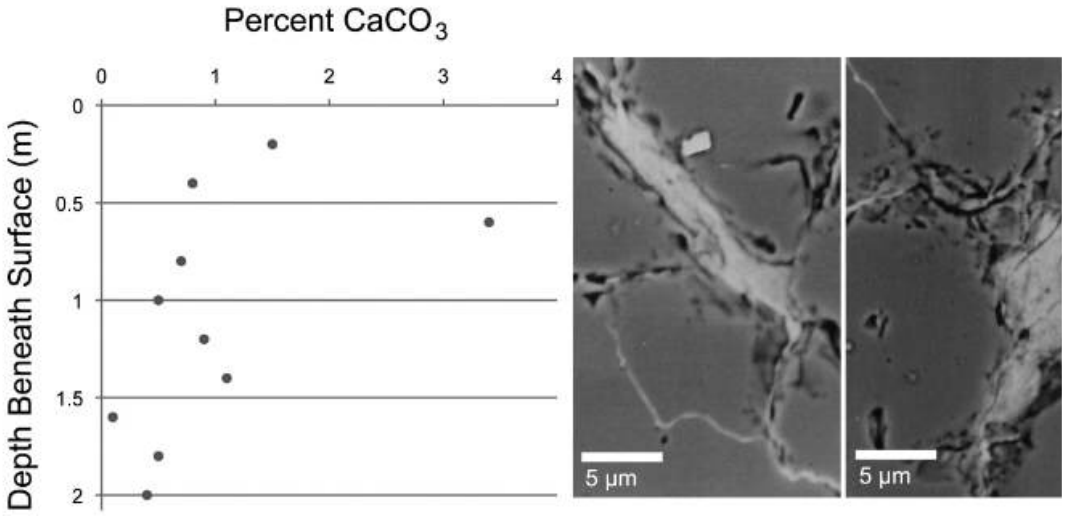

Figure 8. Percent calcium carbonate in micron-scale veins at the Las Sendas site. Each value on the graph represents the cumulative calculation of veins in an area of about 1 mm^2. The two BSE images show typical views of the carbonate found in micron-scale veins in samples that showed no visual evidence of impregnation with calcium carbonate.

BSE CARBONATE TEXTURES

The qualitative investigation of the carbonate veins using BSE to image samples collected at depth of a meter from each site revealed a wide range of

textures. Figure 7 presents a few of the observed textures that include evidence of ongoing silica substitution for carbonate (Figs. 7A and 7B), the encapsulation of silicate silt by laminar calcrete (Fig. 7C), and granular-textured carbonate with considerable variability in porosity (Fig. 7D). This is observed elsewhere in field-studies (*Durand et al., 2007*).

The textures observed in Figures 7-9 explain why percents of carbon in these veins were considerably less than the theoretical value of 12% for $CaCO_3$, and why densities tended to be lower than the expected 2.71 g/cm^{-3} for calcite. The back-scattered electron microscope images demonstrate that detrital pieces of quartz and other silicates occur in with the carbonate in the veins. Also, silica substitution of carbonate occurs to varying degrees at different sites.

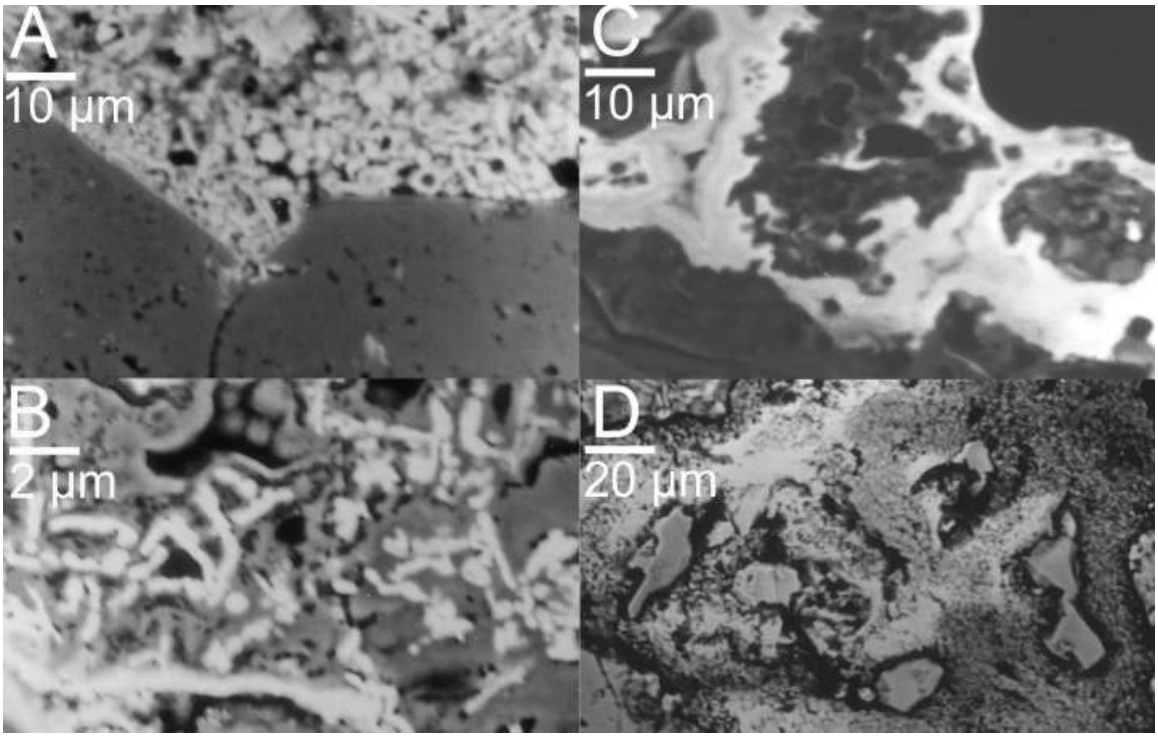

Figure 9. BSE imagery of BFFCs shows evidence of silica replacement, from the site in Figure 3. Image A shows the carbonate (bright, higher Z) adjacent to quartz (darker gray scale, lower Z). The brighter carbonate has a granular texture that is mixed with darker areas of silica. Note the pores in the quartz. We speculate that silica mobilized from the quartz is substituting for the carbonate with ongoing movement of capillary water. Image B reveals a mixing of silica (darker areas) and carbonate (brighter granular linear features). We interpret this texture as calcium carbonate being replaced with silica. Image C shows silt-sized silicate particles (darker) that appear to be encapsulated by carbonate (bright); the quartz wall of the vein is in the lower left. Image D shows a transition from less porous (lighter) carbonate on the left to more porous carbonate on the right. Silt fragments of quartz intermix with the carbonate.

RADIOCARBON RESULTS

Two pilot samples analyzed for radiocarbon dating provide evidence for carbonate mobility in the last glacial period. Samples collected at depths of 0.4 m and 0.8 m in a carbonate vein in the Gila Range excavation (**Fig. 6**) revealed the following:

At 0.4 m depth: 12120±50 BP (Beta 322776) 13C/12C -5.9 o/oo

At 0.8 m depth: 22680±90 BP (Beta 322775) 13C/12C -9.2 o/oo

These radiocarbon measurements have calibrated ages of ~14 ka and ~27 ka.

These data suggest that the carbonate precipitated when the Sonoran Desert around this site hosted a pygmy conifer woodland *(Allen, Swetnam, & Betancourt, 1998)*; *(McAuliffe & Van Devender, 1998)*; *(Van Devender, Thompson, & Betancourt, 1987)*. It is conceivable that a pulse of intense wetness resulted in the transport and precipitation of the dated laminar carbonate (Fig. 7) to depths of 0.8 and 0.4 m. An alternative interpretation is that water moved along the sidewalls of the vein and simply remobilized and reprecipitated pre-existing carbonate that was initially deposited long before the last glacial period. Either explanation would require a far wetter period that exists at the present time.

SR ISOTOPE RESULTS

The concentration of ^{85}Rb, ^{84}Sr, ^{86}Sr, ^{87}Sr, and ^{88}Sr were measured with the Thermo Neptune MC-ICP-MS. The $^{86}Sr/^{87}Sr$ ratios measured are presented in Table 3. An unresolved issue with the sample introduction system is reflected in a deviation from the known values of the standards that were analyzed. While it is unlikely that this issue substantially interrupts the trends collected by the analysis, these data will remain unpublished until a correction can be made.

Table 3. $^{86}Sr/^{87}Sr$ ratios from the Marketplace roadcut.

Sample Code	Sample description	$^{86}Sr/^{87}Sr$	Depth of sample	Known value (standards)
G R1	Gneiss Replicate 1, HCl leached	**0.71135**	**1m**	
G R2	Gneiss Replicate 2, HCl leached	**0.71093**	**1m**	
G R3	Gneiss Replicate 3, HCl leached	**0.71116**	**1m**	
G UL	Gneiss Replicate 4, no HCl leaching	**0.71189**	**1m**	
GSC MG	Gneiss Leachate Carbonate, combined from GR1, GR2 and GR3	**0.70878**	**1m**	
SAC V1	BFFC vein, 30 cm into the exposed face	**0.71335**	**1m**	
G SZ	Gneiss, HCl leached	**0.71056**	**2m**	
GSC SZ	Gneiss Leachate Carbonate	**0.70849**	**2m**	
SAC V2	BFFC vein, 30 cm into the exposed face	**0.71037**	**2m**	
G LP	Gneiss, HCl leached	**0.71287**	**3m**	
GSC LP	Gneiss Leachate Carbonate	**0.72448**	**3m**	
SAC V3	BFFC vein, 30 cm into the exposed face	**0.71046**	**3m**	
G2	U.S.G.S. granite standard (Balcaen, De Schrijver, Moens, & Vanhaecke, 2004)	**0.71207**	**Standard**	**0.709833**
SRM987	Standard run for the mass spectrometer	**0.71079**	**Standard**	**0.71025-0.71030**
SRM987	Standard run for the mass spectrometer	**0.71058**	**Standard**	**0.71025-0.71030**

Table 3 presents the $^{86}Sr/^{87}Sr$ ratios of all samples and standards. Samples of gneiss ranged from 0.71056-0.71287. The leachate carbonate, representing dust infused into fractures in the gneiss, had ratios of 0.70849 and 0.70878. One sample of leachate carbonate was likely contaminated and returned a high rubidium concentration and a ratio of 0.72448, higher than any of the gneiss samples. The carbonate vein material had ratios ranging from 0.71037-0.71335. With exception to the sample of leachate carbonate, the three different materials produced ranges with reasonably proximate values.

Chapter 4

DISCUSSION

ASSESSING BIAS IN OBSERVED VALUES OF STORED CARBON

There are three reasons why the mTC/m^2 amounts reported in Table 2 are likely minimum values for each of the study sites. First, BFFCs continue into bedrock fractures deeper than the 2 m analyzed here (e.g. Figs 2, 5, 6). Second, the BFFCs are often quite friable and erode exposure faces over time, as indicated by the revisitation study in section 4.3. The third reason why our reported values would be minimums is that BFFCs exist at a variety of scales — from veins many centimeters wide down to micrometer widths. Since the methods we used here only mapped veins thicker than about 3 mm, the BFFCs in the thinnest veins are not included in Table 2. The BSE study of one site reported in section 4.4 suggests that micro-veins represented about 1% of the rock volume. Thus, it is likely that the observed mTC values for studied sites in Table 2 are minimum estimates.

THE POTENTIAL SIZE OF THE BFFC CARBON RESERVOIR

For the sake of assessing the potential significance of the global BFFC carbon pool we calculated global pools that likely exist — if other arid and semi-arid regions have similar BFFC carbon content as our study sites in the Sonoran and Mojave Deserts. While we acknowledge this is a giant assumption, that has no support at the present time, these deserts reflect a mix of bedrock types in

mostly arid settings that include cold-season and bimodal precipitation regimes. Thus, we carry out this potential size estimate as an intellectual exercise to be revised as more data becomes available.

Meigs calculated that the world's arid and semi-arid deserts consist of 46.7 million km^2 or 4.67 x 10^{13} m^2 *(Meigs, 1953)*. Goudie tabulates that desert mountains occupy 38%, 43%, 39%, and 47% of the southwestern USA, Saharan, Libyan, and Arabian deserts (*Goudie, 2003*). Hurley et al. present similar values for bedrock highlands of 47%, 43%, and 16% for the Arabian, Saharan and Australian warm deserts *(Hurley, Welte, King, Gilewitch, & Brockhaus, 2004)*. A weighted average based on the area of these deserts generates an approximate figure of 40% of arid and semi-arid regions occupied by mountain ranges.

Multiplying 0.079 ± 0.024 mT mT C/m^2 (Table 2) by 1.87 x 10^{13} m^2, or a rough approximation for the area of desert mountains in arid and semi-arid regions, suggests that there could potentially be 1485±112 GtC of stored carbon in the upper 2 m of desert mountains world-wide. This value is roughly similar to the world's pool of soil organic carbon (Table 4).

Table 4. Estimate of carbon stored in the upper 2 meters of desert mountains, compared with other reservoirs.

Reservoir	Quantity (Gt)
Lithosphere Carbonates	>60,000,000
Lithosphere Kerogens	15,000,000
Oceans Inorganic	37,400
Soil organic carbon (both active and old)	1600
Inorganic carbon mobilized into desert mountains	1370 - 1600
Soil inorganic carbon	780 - 940
Terrestrial Dead Biomass	1200
Oceans Surface	900
Terrestrial Living Biomass	500 - 1000
Atmosphere	800
Soil Litter and Peat	190-230
Aquatic Biomass	1-3

Note: The quantity in Gt derives from multiple sources [*Eswaran et al*., 1993; *Eswaran et al*., 1999; *Falkowski et al*., 2007; *Lal*, 2004; 2008; *Schlesinger*, 1982; *Sundquist*, 1993], as well as this paper.

There are three reasons why the ca. 1485 GtC estimate could be a minimum. First, there is a substantive difference between the estimated planimetric area of desert mountains (*Goudie, 2003*); *(Hurley et al., 2004)* and the much larger surface area of mountain slopes. Second, hyperarid deserts could potentially contain BFFCs. The second author observed two metasedimentary rock excavations containing 4-6% BFFCs in southern coastal Peru. However, hyperarid mountains are not included in our calculations, because the age of the cuts were unknown and two sites do not justify including hyperarid mountains in a global estimate. Third bedrock pediments are relatively flat landforms (*Dohrenwend & Parsons, 2009*) and are not included in estimates of the area of deserts occupied by mountains, because geomorphologists do not consider pediments to be mountains. However, for the purposes of estimating this carbon pool, pediments certainly add to the total area of bedrock-atmosphere interface;

we are unaware of a reasonable estimate for the area of arid bedrock pediments globally. No estimates exist for the global area of bedrock pediments found in arid and semiarid lands. Thus, adding in the area of pediments would increase the global estimate of carbon in the BFFC pool.

There are also reasons why the ca. 1485 GtC estimate could be too high. First, the Sonoran and Mojave sites are dominated by plutonic and metamorphic lithologies, rather than sedimentary or extrusive rock types, and it is possible that the intense jointing at the studied excavations could enhance carbonate penetration into bedrock. Second, the studied sites are located mostly in arid environments and a better representation of semi-arid sites could reveal a lower abundance of carbonate. Third, the studied sites are located in settings that have experienced subsurface rock decay prior to subaerial exposure; it is possible that this "pre-weathered" state could enhance BFFC penetration. Fourth, the area of carbonate mountain ranges would have to be subtracted, if additional studies reveal that the BFFCs in limestone and dolomite derive from the remobilization from fracture walls. Fifth, the studied sites are located in settings that experience dust storms that contain carbonate dust; it is possible that other locales that experience fewer dust storms would host lower values of BFFCs.

CONFOUNDING FACTORS IN ISOTOPE ANALYSIS

The results of this analysis are preliminary. The sample set is too small for statistical analysis. The standards deviated from their known values by a maximum of 0.002, two orders of magnitude off the desired accuracy. These data

will be re-analyzed after mechanical errors have been corrected; however, my laboratory director collaborator and I do not expected that the results of re-analysis will be changed substantially. Additional confounding factors are complied in Table 5.

Table 5. Potential confounding factors in analyzing results of Sr analysis

Confounding Factor	Discussion
Age of the vein carbonate	Sr isotopic ratio of allochthonous sources (eg. dust, meteoric water) at the time of carbonate emplacement into fractures is unknown, and thus cannot be compared to the isotopic ratio of the carbonate
Ratios of modern dust	Sr isotope ratio of dust is not measured directly, by capturing aerosols. It is possible that the ratios derived from the leachate represent unknown influences
Alteration by percolating water	Isotope ratios of vein carbonate could have been influenced by meteoric water percolating down fractures after deposition
Enrichment subsequent to deposition	The carbonate could have had a less radiogenic signal at the time of deposition and become subsequently enriched by weathering of the encasing gneiss

POTENTIAL SOURCES TO THE BFFC CARBON RESERVOIR

Although preliminary, these findings suggest that a significant proportion of the BFFC carbonate could derive from the gneiss. This initial assessment derives from a qualitative comparison of the preliminary results (Table 6). The gneiss was generally the most radiogenic in nature, followed by the vein carbonate, with the leachate carbonate being the least radiogenic of the sample types. Columns five and six show the difference between $^{86}Sr/^{87}Sr$ ratios of the vein carbonate and the gneiss, and the vein carbonate and leachate carbonate respectively. The difference between the vein carbonate and leachate carbonate

was at least twice as great and at most an order of magnitude greater than the difference between the vein carbonate and the gneiss.

Table 6. Data from Table 3, reorganized to facilitate comparisons

Depth	86Sr/87Sr of Gneiss	86Sr/87Sr of Carbonate Veins (30 cm depth into road cut)	86Sr/87Sr of Carbonate Leached From Gneiss (roadcut surface)	d gneiss (BFFC-Gneiss)	d dust (BFFC-gneiss leachate)	Order of Difference between Fracture Carbonate and Potential Source
1 m	0.71115	0.71335	0.70878	0.0022	0.00457	2x
2 m	0.71056	0.71037	0.70849	-0.00019	0.00188	10x
3 m	0.71287	0.71046	0.72448	-0.00241	-0.01402	5-6x

It is reasonable to assume that the isotopic ratio of the leachate carbonate is generally reflective of the composition of modern aerosols — which in turn combine deflated Quaternary deposits and modern contributions. The large disparity between the isotopic ratio of the vein carbonate and the leachate carbonate indicates that contemporary dust — some mix of deflated Quaternary soils and modern sources — is not a source for the carbonate veins. Radiocarbon dating suggests a minimum residence of about 12,000 calendar years for the near surface carbonate veins. No existing data suggests that the carbonate dust in circulation 12 ka would have drastically different isotopic ratios than modern dust.

The isotopic ratios obtained for the leachate carbonate and the vein carbonate are similar to results obtained by Chiquet et al. (1999) (see Fig. 1D). They observed a continuous laminar horizon of carbonate overlaying a discontinuous horizon where carbonate appeared as veins infilling fractures. They sampled carbonate from the vertical profile at a range of depths (0.25-3.8 m) and

found the samples were increasingly radiogenic with depth (Fig. 10). Chiquet et al found the local gneissic bedrock had an isotopic ratio significantly different than the carbonate, such that the *maximum* contribution to the carbonate from bedrock weathering is 33.5%. At South Mountain, the isotope ratios of the vein carbonate and the bedrock are more similar, which could suggest an even higher weathering contribution than those found by Chiquet et al. working in Spain.

Type/N° Sample	Sample description	Depth (cm)	$CaCO_3$	$^{87}Sr/^{86}Sr$	±	[Sr]	[Ca
a - Carbonates*			g/cm^3				
19-95	Transition CRBH/CCH: laminated structure	45–25	0.83	0.710168	*21*	285	3
18-95	Continuous calcrete horizon	50–70	0.85	0.709857	*21*	188	5
15-95	Continuous calcrete horizon	70–60	0.90	0.709744	*21*	192	4
14-95	Continuous calcrete horizon	100–80	0.66	0.709827	*14*	364	2
13-95	Reddish carbonate (presence of clays)	75–55	0.71	0.710271	*22*	225	3
12-95	Continuous calcrete horizon	95–75	0.81	0.709610	*23*	593	1
11-95	Continuous calcrete horizon	110–90	0.58	0.709875	*22*	439	2
10-95	Continuous calcrete horizon	150–130	0.42	0.709784	*17*	808	1
9-95	Discontinuous Carbonate vein	180–160	0.05	0.710254	*20*	120	5
8-95	Discontinuous calcrete: Carbonate vein	225–205	0.03	0.709913	*22*	654	1
7-95	Discontinuous calcrete: Carbonate vein	235–255	0.07	0.710110	*23*	194	4
5-95	Discontinuous calcrete: Carbonate vein	300–280	0.01	0.710369	*22*	100	7
4-95	Discontinuous calcrete: Carbonate vein	320–300	0.07	0.710125	*23*	127	7
3-95	Discontinuous calcrete: Carbonate vein	340–320	0.02	0.710273	*23*	170	5
2c-95	Discontinuous calcrete: Carbonate vein	380–360	0.03	0.710553	*22*	85	8
2b-95	Discontinuous calcrete: Carbonate vein	380–360	0.03	0.710594	*107*	498	1
2a-95	Discontinuous calcrete: Carbonate vein	380–360	0.02	0.710278	*18*	127	6

Figure 10. Screen shot capturing depth vs. isotopic ratio values for carbonate from "Table 1 87Sr/86Sr ratios, [Sr] (ppm), and molar [Ca]/[Sr] ratios for the calcrete profile, local groundwater, rainfall and dust (1995–1996)." (Chiquet et al., 1999)

Strontium isotopic ratios of carbonates range substantially depending on inputs. (*Naiman, Quade, & Patchett, 2000*), for example, found Sr isotope ratios within the range found for vein carbonates at South Mountain in eolian-derived laminar and surface carbonates. However, the similarity between the isotopic ratio of the South Mountain gneiss and the vein carbonate likely suggests substantial contribution by weathering to the carbonate accumulation. If this is true the mineralization process sequestered atmospheric CO_2 now contained in the

accumulation. Erosion and the subsequent exposure of the carbonate to dissolution would re-release this CO_2 acting as a source on Quaternary timescales.

EVALUATING THE MASS BALANCE OF BFFCS

In our conceptual thinking, the mass of BFFCs is a balance of carbonate insertion into the fractures by precipitation and removal by erosion of the bedrock surface. During the Holocene the southwestern United States has maintained consistently low levels of precipitation. The radiocarbon date obtained on an upper BFFC horizon would suggest that BFFCs at this Sonoran Desert site has not received notable input for the past ~14,000 years. The ^{14}C ages we obtained are in the range of those obtained by Whelan et al. (1994) of 21-45 from the upper carbonate veins at Yucca Mountain.

BFFCs mass balance has probably experienced a net loss over the arid Holocene period because input is likely to be dependent on high levels of precipitation, such as the 190-200 ka phase of carbonate deposition in South India (*Durand et al., 2007*). Further radiocarbon dating of upper BFFC surfaces at other sites could reveal more recent deposition, but available data suggests that carbonates in the BFFCs could relate to precipitation during wetter periods. Unlike soil systems that are reactive on centennial timescales, BFFC deposits represent either a slow accumulation of carbonate or carbonate flushed into the system in pulses with climate. We speculate that deeper deposits could be relics of particularly intense wet periods or even wet phases of the Pliocene.

To estimate the average rate of release or carbonate from bedrock, we turn to six studies that report rates of erosion of bedrock and of pediments in arid regions (Bierman & Caffee, 2001); *(Decker, Niedermann, & De Wit, 2011)*; *(Heimsath, Chappell, Dietrich, Nishiizumi, & Finkel, 2001)*; *(Hunt & Wu, 2004)*; *(Kounov et al., 2007)*; *(Nichols et al., 2005)* that all report consistently low rates of erosion, from 1.1-9.5mm/ka in bedrock and from 22-100 mm/ka in pediments. Based on the estimate of ~1485 GtC stored in BFFCs in the upper two m, the upper mm of the bedrock horizon could contain ~0.74 GtC, although this value is probably higher because carbonate concentration tends to decrease with depth. Based on the erosion rates estimated for desert bedrock (Table 7), incremental erosion of bedrock has stripped and exposed a maximum of 74 GtC and a minimum 0.814 GtC over the past ka.

Table 7. Compilation of rates of erosion of bedrock in desert mountains and pediments

Study	Location	Average rate of bedrock erosion
[*Kounov et al.*, 2007]	South African escarpment	1.5-3 mm/ka
[*Bierman and Caffee*, 2001]	Namib desert	1.1-7.5 mm/ka
[*Nichols et al.*, 2005]	Mojave desert	21-100 mm/ka
[*Hunt and Wu*, 2004]	Mojave desert	31 mm/ka
[*Heimsath et al.*, 2006]	Southeastern Australia	9 mm/ka 22 mm/ka
[*Decker et al.*, 2011]	South Africa	2.5 mm/ka

Liu et al. (2010) published a synopsis of recent research challenging the idea that the weathering of silicate minerals is the principal regulator of

atmospheric carbon on geologic timescales, suggesting that the role of carbonate weathering in the drawdown and sequestration of carbon has been greatly underestimated: "the atmospheric CO_2 sink by carbonate weathering contributes about 94% to the atmospheric CO_2 sink, while only 6% results from silicate weathering." The weathering of carbonate minerals increases alkalinity in the water cycle, and increases the CO_2 content of in local water systems *(Z. Liu et al., 2010*). If correct, this finding suggests that periods of high precipitation would be associated with an increased flux of CO_2 from the atmosphere into BFFCs and periods of aridity would be associated with release of carbonates from bedrock due to erosion. We can estimate the impact of the Holocene, by extrapolating an erosion rate of 19 mm/ka (the average of rates in **Table 7**) over the past 1400 years of aridity, suggesting a potential release of 22 GtC from BFFC reservoirs. Thus, the amount of BFFC release is relatively a very small player in the exchange of atmospheric carbon (*Sundquist, 1993*) but could contribute ~1.5 GtC per 100 years, representing roughly 0.000025% of the annual carbon flux from terrestrial environments to the atmosphere (annual values of carbon flux from *Falkowski et al*., 2007).

PLACE OF BFFCS IN THE GLOBAL CARBON CYCLE

The initial radiocarbon results reported in section 4.6 indicate remobilization or initial precipitation of BFFCs at one site in the last glacial period ca. 14-27 ka. These findings are similar to ^{14}C ages of 21-45 ka on eleven samples of calcite at Yucca Mountain *(Whelan et al., 1994)*. Given the

radiocarbon data on BFFCs, and the episodic nature of calcite deposition events at Yucca Mountain at 28 ka, 170 ka, and 280 ka recorded by U-series dating (*Szabo & Kyser, 1990*), it is distinctly possible that BFFCs in the Southwestern USA represent carbon stored during glacial periods. While strontium-isotope data on BFFCs is lacking, even if the BFFCs represent recycled carbonate from dust, the carbon stored in desert bedrock still represents a substantial quantity of stored carbon dioxide.

Future investigation could elucidate processes that could cause the BFFC carbon pool to behave as a source or sink. Sources of the BFFC carbonate are likely the coupled redistribution of carbonate dust during dry phases and weathering of Ca-bearing silicates, emplaced by meteoric infiltration during wet phases. Wet periods may also dissolve the upper sections of the carbonate veins and redistribute carbonates deeper into the fractures, regenerating isotopic ^{14}C, in which case the true timing of deposition could be substantially earlier than the ages obtained for our pilot samples. Wet climatic periods increasing weathering and the subsequent flux of Ca mobilization results in carbonate formation, and could flush the carbonate into storage in the pre-existing fracture matrix. Various studies have posited episodic deposition concurrent with changes in climate (*Chiquet et al., 1999*); *(Durand et al., 2007)*; *(Szabo & Kyser, 1990)*. According to a study by Durand et al. (2007: 35) "the radiometric ages (of the carbonate) suggest that weathering may occur massively at discrete intervals of geologic history, during spikes of humidity in the paleoclimatic record".

Of equal significance to the carbon budget are questions regarding rates and process of BFFC release. The authors have observed thick veins of carbonate exposed by erosion throughout various mountainsides in south-central Arizona. Due to the minimal soil cover that characterizes arid mountains, exposed BFFCs are rapidly dissolved and physically weathered. BFFCs likely experience some *in situ* dissolution, and movement towards nearby gullies. In pediment systems, Horton overland flow dissolves and re-precipitates carbonate as coatings on alluvial deposits and on gully walls, and could access the uppermost BFFC horizon. Pedimentation of bedrock slopes is ubiquitous in arid and semi arid regions *(Parsons, Abrahams, & Howard, 2009)*. Rates of slope erosion have been recently described with various numerical models (*Heimsath, Deitrich, Nishiizumi, & Finkel, 1997)*; *(Hunt & Wu, 2004)*; *(Pelletier, 2010)*; *(Strudley, Murray, & Haff, 2006)* and with field samples from pediments *(Gunnell, Braucher, Bourles, & Andre, 2007); (Heimsath, Chappell, Dietrich, Nishiizumi, & Finkel, 2006; Kounov et al., 2007)*; *(Nichols et al., 2005)* and bedrock exposures (*Bierman & Caffee, 2001*); *(Decker et al., 2011)*. These rates for soil production and erosion imply the Quaternary rate at which BFFCs are exposed to physical and chemical weathering.

Bedrock fractures that store carbonate over the long term are not likely to play a role in attempts to sequestrate carbon *(McPherson & Sundquist, 2009)*. The geological potential to store 3400 GtC (*Sundquist et al., 2008*) far exceeds the amount currently found in BFFCs. However the significance of this pool of desert bedrock carbon could be similar to pedogenic carbonate. Alternatively,

our speculative hypothesis is that BFFCs represent carbon stored in what are now arid mountains during the late Pliocene and the wettest phases of the Pleistocene, when regular moisture penetration could reach meters into bedrock fractures. If this speculation is valid, BFFCs could have played a role influencing global climate change on late Pliocene *(Lunt, Foster, Haywood, & Stone, 2008*); *(Seki et al., 2010)* and Pleistocene (*Paces et al., 2010*); *(Vaniman & Chipera, 1996)*, p. 4418 timescales.

CONCLUSION

Models of terrestrial carbon pathways tend to focus on biotic systems as the principal mechanism removing CO_2 from the atmosphere. The Earth's bedrock skin has been neglected as an actor in atmospheric CO_2 budgets. However, our initial research demonstrates that arid and semi-arid mountains could potentially be storing carbonate with a magnitude on the order of soil inorganic carbon. Our study coupled with the thinking of Liu et al. [2011] and others suggests semi-arid and arid bedrock ranges could be important players in terrestrial accumulation of carbonate.

REFERENCES

Allen, C., Swetnam, T., & Betancourt, J. (1998). Landscape changes in the southwestern united states: Techniques, long-term data sets, and trends. In T. D. Sisk (Ed.), *Perspectives on the land use history of north america: A context for understanding our changing environment. U.S. Geological survey biological resources division, biological science report usgs/brd/bsr-1998-0003. See also http://biology.Usgs.Gov/luhna/chap9.Html* (pp. 104). Reston: U.S. Geological Survey.

Amundson, R. G., Richter, D. D., Humphreys, G. S., Jobbagy, E. G., & Gaillardet, J. (2007). Coupling between biota and earth materials in the critical zone. *Elements, 3*, 327-332.

Bathurst. (1972). *Carbonate sediments and their diagensis*. Amsterdam: Elsevier.

Berner, R. A. (2003). The long-term carbon cycle, fossil fuels and atomospheric carbon. *Nature, 426*, 323-326.

Bierman, P. R., & Caffee, M. (2001). Slow rates of rock surface erosion and sediment production across the namib desert and escarptment, southern africa. *American Journal of Science, 301*(4-5), 326.

Bish, D. L., & Aronson, J. L. (1993). Paleogeothermal and paleohydrologic conditions in silicic tuff from yucca mountain, nevada. *Clays and Clay Minerals, 41*(2), 148-161.

Bish, D. L., & Chipera, S. J. (1989). Revised mineralogic summary of yucca mountain, nevada: Los Alamos National Lab, NM.

Brantley, S., Goldhaber, M. B., & Ragnarsdottir, K. V. (2007). Crossing disiplines and scales to understand the critical zone. *Elements, 3*, 307-314.

Callen, R. A., Wasson, R. J., & Gillespie, R. (1983). Reliability of radiocarbon dating of pedo- genic carbonate in the australian arid zone. *Sedimentary Geology, 35*, 1-14.

Candy, I., Black, S., Sellwood, B. W., & Rowan, J. S. (2003). Calcrete profile development in quaternary alluvial sequences, southeast spain: Implications for using calcretes as a basis for landform chronologies. *Earth Surface Processes and Landforms, 28*, 169-185.

Capo, R. C., & Chadwick, O. A. (1999). Sources of strontium and calcium in desert soil and calcrete. *Earth and Planetary Science Letters, 170*(1-2), 61-71. doi: 10.1016/S0012-821X(99)00090-4

Capo, R. C., Whipkey, C. E., Blachere, J. R., & Chadwick, O. A. (2000). Pedogenic origin of dolomite in a basaltic weathering profile, kohala peninsula, hawaii. *Geology, 28*(3), 271-274.

Carlos, B. A., Chipera, S. J., Bish, D. L., & Craven, S. J. (1993). Fracture-lining manganese oxide minerals in silicic tuff, yucca mountain, nevada, u.S.A. *Chemical Geology, 107*, 47-69.

Chiquet, A., Michard, A., Nahon, D., & Hamelin, B. (1999). Atmospheric input vs in situ weathering in the genesis of calcretes: An sr isotope study at galvez (central spain). *Geochimica Cosmochimica Acta, 63*, 311-323.

Chitale, J. D. (1986). *Study of petrography and internal structures in calcretes of west texas and new mexico (microtextures, caliche). Ph.D. Dissertation*. Thesis, Texas Tech University, Lubbock.

Dart, R. C., Barovich, K. M., Chittleborough, D. J., & Hill, S. M. (2007). Calcium in regolith carbonates of central and southern australia: Its source and implications for the global carbon cycle. *Palaeogeography, Palaeoclimatology, Palaeoecology, 249*, 322-334.

Decker, J. E., Niedermann, S., & De Wit, M. J. (2011). Soil erosion rates in south africa compared with cosmogenic 3he-based rates of soil production. *South African Journal of Geology, 114*(3-4), 475-488.

Denniston, R. F., Shearer, C. K., Layne, G. D., & Vaniman, D. T. (1997). Sims analyses of minor and trace element distributions in fracture calcite form yucca mountain, nevada, USA. *Geochimica Cosmochimica Acta, 61*(9), 1803-1818.

Derry, L. A., & Chadwick, O. A. (2007). Contributions from earth's atmosphere to soil. *Elements, 3*, 333-338.

Diaz-Hernandez, J. (2010). Is soil carbon storage underestimated? *Chemosphere, 80*, 346-349.

Dohrenwend, J. D., & Parsons, A. J. (2009). Pediments in arid environments. In A. J. Parsons & A. D. Abrahams (Eds.), *Geomorphology of desert environments* (pp. 377-411). New York: Springer.

Dorn, R. I. (1995). Digital processing of back-scatter electron imagery: A microscopic approach to quantifying chemical weathering. *Geological Society of America Bulletin, 107*, 725-741.

Durand, N., Gunnell, Y., Curmi, P., & Ahmad, S. M. (2006). Pathways of calcrete development on weathered silicate rocks in tamil nadu, india: Mineralogy, chemistry and paleoenvironmental implications. *Sedimentary Geology, 192*, 1-18.

Durand, N., Gunnell, Y., Curmi, P., & Ahmad, S. M. (2007). Pedogenic carbonates on precambrian silicate rocks in south india: Origin and paleoclimatic significance. *Quaternary International, 162-163*, 35-49.

Eswaran, H., Reich, P. F., Kimble, J. M., Beinroth, F. H., Padmanabhan, E., & Moncharoen, P. (1999). Global carbon stocks. In R. Lal, J. M. Kimble, H. Eswaran & B. A. Stewart (Eds.), *Global climate change and pedogenic carbonates* (pp. 15-25). Boca Raton: Lewis Publishers.

Eswaran, H., Van den Berg, E., & Reich, P. (1993). Organic carbon in soils of the world. *Soil Science Society of America Journal, 57*, 192-194.

Falkowski, P., Scholes, R. J., Boyle, E., Canadell, J., Canfield, D., Elser, J., . . . Steffen, W. (2007). The global carbon cycle: A test of our knowledge of earth as a system. *Science, 290*, 291-296.

Fletcher, K. E. K., Rockwell, T. K., & Sharp, W. D. (2011). Late quaternary slip rate of the southern elsinore fault, southern california: Dating offset alluvial fans via 230th/u on pedogenic carbonate. *Journal of Geophysical Research, 116*, F02006, doi:02010.01029/02010JF001701.

Goldstein, J., Newbury, D. E., Joy, D. C., Lyman, C. E., Echlin, P., Lifshin, E., . . . J.R, M. (2003). *Scannign electron microscopy and x-ray microanalysis*. Amsterdam: Elsevier.

Goudie, A. S. (2003). *Great warm deserts of the world: Landscapes and evolution*. New York: Oxford University Press.

Gunnell, Y., Braucher, R., Bourles, D., & Andre, G. (2007). Quantitative and qualitative insights into bedrock landform erosion on the south indian craton using cosmogenic nuclides and apatite fission tracks. *GSA Bulletin, 119*(5/6), 576-585.

Hamidi, E. M., Colin, F., Michard, A., Boulange, B., & Nahon, D. (2001). Isotopic tracers of the origin of ca in a carbonate crust from the middle atlas, morocco. *Chemical Geology, 176*, 93-104.

Hamidi, E. M., Geraud, Y., Colin, F., & Boulange, B. (1999). Analyse de la porosite dans un profil d'encroutment carbonate sur les basaltes du trias du moyen atlas (maroc). *Comptes Rendus de l'Académie des Sciences de la terre et des planetes, 329*, 351-356.

Heilweil, V. M., McKinney, T. S., Zhdanov, M. S., & Watt, D. E. (2007). Controls on the variability of net infiltration to desert sandstone. *Water Resources Research, 43*, 1-15 (W07431, doi:07410.01029/02006WR005113).

Heimsath, A. M., Chappell, J., Dietrich, W. E., Nishiizumi, K., & Finkel, R. C. (2001). Late quaternary erosion in southeastern australia: A field example using cosmogenic nuclides. *Quaternary International, 83-85*, 169-185.

Heimsath, A. M., Chappell, J., Dietrich, W. E., Nishiizumi, K., & Finkel, R. C. (2006). Soil production on a retreating escarpment in southeastern australia. *Geology, 28*, 787-790.

Heimsath, A. M., Deitrich, W. E., Nishiizumi, K., & Finkel, R. (1997). The soil production function and landscape equilibrium. *Nature, 388*, 358-361.

Hill, S. M., Taylor, G., & McQueen, K. G. (1998). Genesis of some calcretes in the southern yilgarn craton, western australia: Implications for mineral exploration—discussion. *Australian Journal of Earth Sciences, 45*, 177–178.

Hunt, A. G., & Wu, J. Q. (2004). Climatic influences on holocene variations in soil erosion rates on a small hill in the mojave desert. *Geomorphology, 58*, 263-289.

Hurley, B., Welte, S., King, W., Gilewitch, D., & Brockhaus, J. (2004). *Desert analysis: The quest for training areas*. West Point, NY: Center for Environmental and Geographical Sciences, United States Military Academy.

Jacobson, A. D., Blum, J. D., & Walter, L. M. (2002). Reconciling the elemental and sr isotope composition of himalayan weathering fluxes: Insights from the carbonate geochemistry of stream waters. *Geochimica Cosmochimica Acta, 66*(19), 3417-3429.

Klappa, C. F. (1979). Lichen stromatolites: Criterion for subaerial exposure and a mechanism for the formation of laminar calcretes (caliche). *Journal of Sedimentary Petrology, 49*, 387-400.

Knauth, L. P., Brilli, M., & Klonowski, S. (2003). Isotope geochemistry of caliche developed on basalt. *Geochimica Cosmochimica Acta, 67*, 185-195.

Kounov, A., Niedermann, S., De Wit, M. J., Viola, G., Andreoli, M., & Erzinger, J. (2007). Present denundation rates at selected sections of the south african escarpment and the elevated continental interior based on cosmogenic 3he and 21ne. *South African Journal of Geology, 110*, 235-248.

Krinsley, D. H., & Manley, C. R. (1989). Backscattered electron microscopy as an advanced technique in petrography. *Journal of Geological Eduction, 37*, 202-209.

Lal, R. (2004). Soil carbon sequestration impacts on global climate change and food security. *Science, 304*, 1623-1627.

Lal, R. (2008). Sequestration of atmospheric co2 in global carbon pools. *Energy & Environmental Science, 1*, 86-100.

Lerman, A., & MacKenzie, F. T. (2005). Co2 air-sea exchange due to calcium carbonate and organic matter storage, and its implications for the global carbon cycle. *Aquatic Geochemistry, 11*, 345-390.

Liu, S., Bliss, N., Sundquist, E. T., & Huntington, T. G. (2003). Modeling carbon dynamics in vegetation and soil under the impact of soil erosion and deposition. *Global Biogeochemical Cycles, 17*(2), 43-41 - 43-42.

Liu, Z., Dreybrodt, W., & H., L. (2011). Atmospheric co2 sink: Silicate weathering or carbonate weathering? *Applied Geochemistry, 26*, S292-S294.

Liu, Z., Dreybrodt, W., & Wang, H. (2010). A new direction in effective accounting for the atmospheric co1 budget: Considering the combined action of carbonate dissolution, the global water cycle and photosynthetic uptake of dic by aquatic organisms. *Earth-Science Reviews, 99*, 162-172.

Lunt, D. J., Foster, G. L., Haywood, A. M., & Stone, E. J. (2008). Late pliocene greenland glaciation controlled by a decline in atmospheric co2 levels. *Nature, 454*, 1102-1105.

McAuliffe, J. R., & Van Devender, T. R. (1998). A 22,000-year record of vegetation change in the north-central sonoran desert. *Palaeogeography, Palaeoclimatology, Palaeoecology, 141*, 253-275.

McPherson, B. J., & Sundquist, E. T. (Eds.). (2009). *Carbon sequestration and its role in the global carbon cycle*. Washington D.C.: American Geophysical Union.

McQueen, K. G., Hill, S. M., & Foster, K. A. (1999). The nature and distribution of regolith carbonate accumulations in southeastern australia and their potential as a sampling medium in geochemical exploration. *Journal of Geochemical Exploration, 67*, 67-82.

Meigs, P. (1953). World distribution of arid and semi-arid homoclimtes. In A. Z. Programme (Ed.), *Review of research on arid zone hydrology* (Vol. 1, pp. 203-209). Paris: UNESCO.

Moore, C. H. (1989). *Carbonate diagenesis and porosity*. Amsterdam: Elsevier.

Nash, D. J., & McLaren, S. J. (2003). Kalahari valley calcretes: Their nature, origing, and envrionmental significance. *Quaternary International, 111*, 3-22.

Neymark, L. A., Amelin, Y., Paces, J. B., & Peterman, Z. E. (2002). U-pb ages of secondary silica at yucca mountain, nevada: Implications for the paleohydrology of the unsaturated zone. *Applied Geochemistry, 17*, 709-734.

Neymark, L. A., Paces, J. B., Marshall, B. D., Peterman, Z. E., & Whelan, J. F. (2005). Geochemical and c,o,sr, and u-series isotopic evidence for the meteoric origin of calcrete at solitario wash, crater flat, nevada, USA. *Environmental Geology, 48*(4-5), 450-465.

Nichols, K. K., Bierman, P. R., Eppes, M. C., Caffee, M., Finkel, R., & Larsen, J. (2005). Late quaternary history of the chemehuevi mountain piedmont, mojave desert, deciphered using 10be and 26al. *American Journal of Science, 305*, 345-368.

Paces, J. B., Neymark, L. A., Whelan, J. F., Wooden, J. L., Lund, S. P., & Marshall, B. D. (2010). Limited hydrologic response to pleistocene climate change in deep vadose zones — yucca mountain, nevada. *Earth and Planetary Science Letters, 300*, 287-298.

Parsons, A. J., Abrahams, A. D., & Howard, A. D. (2009). Rock-mantled slopes. In A. J. Parsons & A. D. Abrahams (Eds.), *Geomorphology of desert environments* (pp. 233-263). New York: Springer.

Pelletier, J. D. (2010). How do pediments form?: A numerical modeling investigation with comparison to pediments in southern arizona, USA. *GSA Bulletin, 122*(11/12), 1815-1829.

Peterman, Z. E., Stuckless, J. S., Marshall, B. D., Mahan, S. A., & Futa, K. (1992). *Strontium isotope geochemistry of calcite fracture fillings in deep core, yucca mountain, nevada- a progress report*. Paper presented at the High Level Radioactive Wast Management.

Quade, J. (1990). Stable isotopic evidence for a pedogenic origin of carbonates in trench 14 near yucca mountain, nevada. *Science, 250*(4987), 1549-1552.

Quade, J., Chivas, A. R., & MCCulloch, M. T. (1995). Strontium and carbon isotope tracers and the origins of soil carbonate in south australia and victoria. *Palaeogeography, Palaeoclimatology, Palaeoecology, 113*(103-117).

Rasmussen, C. (2006). Distribution of soil organic and inorganic carbon pools by biome and soil taxa in arizona. *Soil Science Society of America Journal, 70*, 256-265.

Reynolds, S. J., & Bartlett, R. D. (2002). Subsurface geology of the easternmost phoenix basin, arizona: Implications for groundwater flow. *Arizona Geological Survey Contributed Report, CR-02-A*, 1-75.

Schlesinger, W. H. (1982). Carbon storage in the caliche of arid soils: A case study from arizona. *Soil Science, 133*, 247-255.

Schlesinger, W. H. (1985). The formation of caliche in soils of the mojave desert, california. *Geochimica et Cosmochimica Acta, 49*, 57-66.

Seki, O., Foster, G. L., Schmidt, D. N., Mackensen, A., Kawamura, K., & Pancost, R. D. (2010). Alkenone and boron-based pliocene pco2 records. *Earth and Planetary Science Letters, 292*, 201-211.

Sombroek, W. G., Nachtergaele, F. O., & Hebel, A. (1993). Amounts, dynamics and sequestering of carbon in tropical and subtropical soils. *Ambio, 22*, 417–426.

Stadelman, S. (1994). *Genesis and post-formational systematics of carbonate accumulations in quaternary soils of the southwestern united states*. Ph.D. Dissertation, Texas Tech University, Lubbock.

Stokes, M., Nash, D. J., & Harvey, A. M. (2006). Calcrete 'fossilisation' of alluvial fans in se spain: The roles of groundwater, pedogenic processes and fan dynamics in calcrete development. *Geomorphology, in press*.

Strudley, M. W., Murray, A. B., & Haff, P. K. (2006). Emergence of pediments, tors, and piedmont junctions from a bedrock weathering-regolith thickness feedback. *Geology, 34*, 805-808.

Stuckless, J. S., Peterman, Z. E., & Muhs, D. R. (1991). U and sr isotopes in ground water and calcite, yucca mountain, nevada: Evidence against upwelling water. *Science, 254*, 5031.

Suchet, P. A., Probst, J., & Ludwig, W. (2003). Worldwide distribution of continental rock lithology: Implications for the atmospheric/soil co2 uptake by continental weathering and alkalinity river transport to the oceans. *Global Biogeochemical Cycles, 17*, 1038, doi:1010.1029/2002GB001891.

Sundquist, E. T. (1993). The global carbon dioxide budget. *Science, 259*, 934-941.

Sundquist, E. T., Ackerman, K. V., Parker, L., & Huntzinger, D. N. (2009). An introduction to global carbon cycle management. In B. J. McPherson & E. T. Sundquist (Eds.), *Carbon sequestration and its role in the global carbon cycle: Geophysical monograph series* (Vol. 183, pp. 1-23): American Geophysical Union.

Sundquist, E. T., Burruss, R. C., Faulkner, S., Gleason, R., Harden, J., Kharaka, Y., . . . Waldrop, M. (2008). *Carbon sequestration to mitigate climate change*. Washington D.C.: U.S. Geological Survey.

Szabo, B. J., & Kyser, T. K. (1990). Ages and stable-isotope compositions of secondary calcite and opal in drill cores from tertiary volcanic rocks of the yucca mountain area, nevada. *Geological Society of America Bulletin, 102*.

Torn, M. S., Trumbore, S. E., Chadwick, O. A., Vitousek, P. M., & Hendricks, D. M. (1997). Mineral control of soil organic carbon storage and turnover. *Nature, 389*, 170-173.

Urey, H. C. (1952). *The planets, their origin and development*. New Haven, Conn.: Yale University Press.

Van Devender, T. R., Thompson, R. S., & Betancourt, J. L. (1987). *Vegetation history of the deserts of southwestern north america; the nature and timing of the late wisconsin-holocene transition*. Boulder, Colo: Geological Society of America.

Vaniman, D. T., & Chipera, S. J. (1996). Paleotransport of lanthanides and strontium recorded in calcite compositions from tuffs at yucca mountain, nevada. *Geochimica Cosmochimica Acta, 60*, 4417-4433.

Vaniman, D. T., & Whelan. (1994). Inferences of paleoenvironment from petrographic, chemical and stable-isotope studies of calcretes and fracture calcites. Report number: La-ur-94-640 conf-940553-13. In T. L. Sanders (Ed.), *High level radioactive waste management 1994. Proceedings of the fifth annual international conference, las vegas, nevada, may 22-26, 1994* (pp. 2730-2737). New York: American Society of Civil Engineers.

Verrecchia, E. P. (1990). Litho-diagenetic implications of the calcium oxalate-carbonate biogeochemical cycle in semiarid calcretes, nazareth, israel. *Geomicrobiology Journal, 8*, 87-99.

Wang, Y., Amundson, R., & Trumbore, S. (1994). A model for soil (co2) c-14 and its implications for using c-14 to date pedogenic carbonate. *Geochimica et Cosmochimica Acta, 58*, 393-399.

Watts, N. L. (1980). Quaternary pedogenic calcretes from the kalahari (southern africa): Mineralogy, genesis and diagenesis. *Sedimentology, 27*, 661-686.

Whelan, J. F., Paces, J. B., & Peterman, Z. E. (2002). Physical and stable-isotope evidence for formation of secondary calcite and silica in the unsaturated zone, yucca mountain, nevada. *Applied Geochemistry, 17*, 735-350.

Whelan, J. F., & Stuckless, J. S. (1992). *Paleohydrologic implications of the stable isotope composition of secondary calcite within yucca mountain, nevada*. Paper presented at the International high level radioactive waste management, Las Vegas, NV.

Whelan, J. F., Vaniman, D. T., Stuckless, J. S., & Moscati, R. J. (1994). *Paleoclimatic and paleohydrological records from secondary calcite: Yucca mountain, nevada*. Paper presented at the High Level Radioactive Waste Management, Las Vegas, NV.

Wilson, N. S. F., Cline, J. S., & Amelin, Y. V. (2003). Origin, timing, and temperature of secondary calcite-silica mineral formation at yucca mountain, nevada. *Geochimica Cosmochimica Acta, 67*, 1145-1176.

Winter, B. L., & Knauth, L. P. (1992). Stable iostope geochemistry of carbonate fracture fills in montery formation, california. *Journal of Sedimentary Research, 62*(2), 208.

APPENDIX A

AUTHOR PERMISSION FOR USE OF DIAGRAMS COMPILED IN FIGURE 1

Permission to use your diagram

11 messages

Ronald Dorn <atrid@asu.edu> 22 May 2012 14:48 To: achiquet@cerege.fr, fcolin@arbois.cerege.fr, durand@cerege.fr, heilweil@usgs.gov, kmq@science.canberra.edu.au
Cc: Emma Harrison <ejharri1@asu.edu>

Dear Drs. Chiquet, Colin, Durand, Heilweil, and McQueen,

Emma Harrison and I are writing a paper entitled "An effort to quantify a terrestrial carbon reservoir in warm desert mountains" for Global Biogeochemical Cycles.

We live in metropolitan Phoenix, Arizona, and construction of roads and houses has exposed a lot of weathered and unweathered bedrock faces. We regularly observe what you have all reported in your publications: fractures that have been filled with carbonate. We have examined 31 cross-sections thus far of 20 sq. meter, and we are finding about 0.08 mTC per square meter of desert mountain surface going down to a depth of only 2 m.

In the introduction of our paper, we would like to acknowledge your outstanding research. In particular, we have noted a certain similarity in your diagrams that all show the presence of fractures filled with carbonate. We have compiled those diagrams into the attached figure.

Emma and I are seeking your permission to use your illustration in what would be our Figure 1, because we think it important to do more than simply refer to these diagrams in the text. We want to emphasize the exciting nature of your contributions and do this with the aid of this compiled visualization.

With great respect,

Ron and Emma Desert Geomorphology Lab School of Geographical Sciences and Urban Planning Arizona State University

2 attachments

Ronald Dorn <atrid@asu.edu>

HarrisonDornFig1.pdf
260K

Ronald Dorn <atrid@asu.edu> To: kmq@canberra.edu.au, ken.mcqueen@canberra.edu.au
22 May 2012 15:03
22 May 2012 19:05

Dear Dr. McQueen,

[Quoted text hidden]

2 attachments

HarrisonDornFig1.pdf
260K

BedrockFracturesFilledCarbonate.jpg
734K

Ken.McQueen <Ken.McQueen@canberra.edu.au> To: Ronald Dorn <atrid@asu.edu>

Dear Ron,

BedrockFracturesFilledCarbonate.jpg
734K

Thanks for your email and interest in regolith carbonate. From our point of you it would be fine for you to use that figure with the acknowledgment. A lot of work was done on carbonates (calcrete) in the Cooperative Research Centre for Landscape, Environments and Mineral Exploration between 1995 and 2008, when the centre finished. A large amount of the work is in CRC LEME Publications and Open File reports, which are still accessible on the Web at http://crcleme.org.au/, but I am not sure for how much longer. Open File Report 200 summarises a study done on calcrete in western NSW. Regolith carbonate or calcrete is widespread around the world in arid and semi arid regions. I was recently in the Kalahari in Botswana and it is quite common there. All the best Cheers Ken [Quoted text hidden]

DURAND Nicolas <nicolas.durand@cea.fr> 23 May 2012 02:01 To: Ronald Dorn

<atrid@asu.edu> Cc: Emma Harrison <ejharri1@asu.edu>
Dear Ron and Emma,
Thank you for your interest in my paper dealing with the weathering of metamorphic bedrock in south India, fractures filled with carbonates and the occurrence of various morphologies of pedogenic carbonates.
Your project seems very exciting, with an impressive field work. Please, keep me informed about the publication of your paper. This is a very positive counterpart of urbanization: the observation of new soil or rock profiles which are usually hidden !
Yes, you can use my illustration. Regards, Nicolas.

_____ Dr. Nicolas Durand Carbon-14 Measurement Laboratory (LMC14) LMC14 / CEA Saclay
Bâtiment 450, porte 4E F-91191 Gif-sur-Yvette Cedex email: nicolas.durand@cea.fr ph: +33-1-69-08-14-06
Ronald Dorn <atrid@asu.edu> To: "Ken.McQueen" <Ken.McQueen@canberra.edu.au>
Dear Ken,
Thank you for your kindness, and also for the heads up at the CRC LEME website. It will take me quite a bit of time to digest your great work.
With my best wishes, Ron
[Quoted text hidden]
Ronald Dorn <atrid@asu.edu> To: DURAND Nicolas <nicolas.durand@cea.fr> Cc: Emma Harrison <ejharri1@asu.edu>
Dear Nicolas,
Thank you for your permission, your very rapid reply, and most especially for your great research. I wish you the best for your continued success. Sincerely,
23 May 2012 08:36
23 May 2012 08:37

HarrisonDornFig1.pdf
260K
Victor M Heilweil <heilweil@usgs.gov>24 May 2012 09:34 To: Ronald Dorn <atrid@asu.edu>
Dear Ronald,
Yes, you have my permission to use our figure - glad to see that your are doing research in this interesting area. Please send me a copy of the paper when it is published.
Regards, Vic
********** Victor Heilweil Research Hydrologist U.S. Geological Survey 2329 Orton Circle
Salt Lake City, UT 84119
heilweil@usgs.gov 801-908 - 5042 **********
From: To: Cc: Date: Subject:
Ronald Dorn <atrid@asu.edu> achiquet@cerege.fr, fcolin@arbois.cerege.fr, durand@cerege.fr, heilweil@usgs.gov, kmq@science.canberra.edu.au Emma Harrison <ejharri1@asu.edu> 05/22/2012 03:48 PM Permission to use your diagram
[Quoted text hidden]
[attachment "BedrockFracturesFilledCarbonate.jpg" deleted by Victor M Heilweil/WRD/USGS/DOI]
[attachment "HarrisonDornFig1.pdf" deleted by Victor M Heilweil/WRD/USGS/DOI]
Ronald Dorn <atrid@asu.edu> To: Victor M Heilweil <heilweil@usgs.gov>
Dear Vic, I appreciate your quick response and your kind words.
I have learned a lot reading your papers. My favorite ones are with Kip Solomon and Dennis Watt. I appreciate your science.
24 May 2012 15:32

Sincerely, Ron
[Quoted text hidden]
Daniel Nahon <nahon@cerege.fr> To: Ronald Dorn <atrid@asu.edu>
Le 23/05/12 20:04, Ronald Dorn a écrit :

[Quoted text hidden]
28 May 2012 10:30
Dear Ron and Emma, Of course, I agree with the use of illustration I have published in collaboration with Mokhtar Hamidi in my Chemical Geology 2001 paper or with Arnaud Chiquet in my 1999 Geochimica paper. I would be happy to receive your own paper after publication.
Sincerely, Daniel Nahon professor Aix-Marseille University
Ronald Dorn <atrid@asu.edu> To: Daniel Nahon <nahon@cerege.fr> Cc: Emma Harrison <ejharri1@asu.edu>
Dear Professor Nahon,
We are most grateful for your time in replying, and we would be delighted to send the paper.
We wish you the best of luck on your continued amazing contributions.
Sincerely,
Ron
[Quoted text hidden]
28 May 2012 14:13